© 2013. Published by The Company of Biologists Ltd | Development (2013) 140, 4776-4787 doi:10.1242/dev.096941

RESEARCH ARTICLE

The *Drosophila* ubiquitin-specific protease Puffyeye regulates dMyc-mediated growth

Ling Li[1], Sarah Anderson[1], Julie Secombe[2] and Robert N. Eisenman[1,*]

ABSTRACT

The essential and highly conserved role of Myc in organismal growth and development is dependent on the control of Myc protein abundance. It is now well established that Myc levels are in part regulated by ubiquitin-dependent proteasomal degradation. Using a genetic screen for modifiers of *Drosophila Myc* (*dMyc*)-induced growth, we identified and characterized a ubiquitin-specific protease (USP), Puffyeye (Puf), as a novel regulator of dMyc levels and function *in vivo*. We show that *puf* genetically and physically interacts with *dMyc* and the ubiquitin ligase *archipelago* (*ago*) to modulate a dMyc-dependent cell growth phenotype, and that varying Puf levels in both the eye and wing phenocopies the effects of altered dMyc abundance. Puf containing point mutations within its USP enzymatic domain failed to alter dMyc levels and displayed no detectable phenotype, indicating the importance of deubiquitylating activity for Puf function. We find that dMyc induces Ago, indicating that dMyc triggers a negative-feedback pathway that is modulated by Puf. In addition to its effects on dMyc, Puf regulates both Ago and its cell cycle substrate Cyclin E. Therefore, Puf influences cell growth by controlling the stability of key regulatory proteins.

KEY WORDS: *Drosophila*, Myc, Deubiquitinase, Growth, Protein degradation

INTRODUCTION

The mammalian *Myc* gene family, comprising *Myc*, *Mycn* and *Mycl*, is known to be crucial for growth and development (Grandori et al., 2000). Myc proteins control multiple cellular processes, including cell growth, proliferation, metabolism and apoptosis, and deregulation of Myc plays an important role in oncogenesis (Dang, 2012). Non-mammalian Myc has been most intensively studied in *Drosophila melanogaster* where the absolute requirement for *Drosophila* Myc (dMyc) (*dm* – FlyBase) function during development has been demonstrated by the fact that *dMyc*-null mutants die at an early larval stage (Gallant, 2006; Pierce, 2004). dMyc is necessary and sufficient to regulate organismal growth through cell-autonomous control of cell size (Bellosta and Gallant, 2010; Gallant, 2009; Gallant et al., 1996; Johnston et al., 1999; Maines et al., 2004; Prober and Edgar, 2001).

Myc transcript and protein abundance are subject to regulation at multiple levels ranging from transcriptional control by numerous mitogenic signaling pathways to extensive post-translational modifications (Hann, 2006; Liu and Levens, 2006; Thomas and Tansey, 2011; Vervoorts et al., 2006). Of particular interest, given the relatively short half-life of Myc proteins, is the post-translational modification of Myc by the ubiquitin system (Müller and Eilers, 2009; Thomas and Tansey, 2011). Protein ubiquitylation is a fundamental and versatile post-translational modification that controls multiple cellular events by marking proteins as substrates for either degradation or non-degradative processing (Bhat and Greer, 2011). In mammals, distinct ubiquitin E3 ligase complexes, including Skp2 and Fbw7, have been reported to influence Myc protein stability and activity (Müller and Eilers, 2009; Thomas and Tansey, 2011).

The *Drosophila* ortholog of Fbw7, Archipelago (Ago) is the only ligase identified thus far as involved in proteasome-mediated ubiquitin-dependent turnover of dMyc proteins (Moberg et al., 2004). Ago mutant alleles were first identified in a genetic screen for regulators of tissue growth in the eye, where it was initially shown to bind and regulate Cyclin E (CycE) levels (Moberg et al., 2001). Later work demonstrated that Ago also physically interacts with dMyc, and controls dMyc stability and biological function (Moberg et al., 2004). Unlike c-Myc, which was shown to have a single Myc BoxI phosphodegron associated with Fbw7 binding, several domains containing putative Ago-interacting motifs were shown in dMyc to mediate Casein kinase 1 (CK1)α-, CK1ε- and GSK3β-dependent protein degradation. Although their link to Ago function has not been precisely established, it is clear that GSK3β plays a key role in Ago-mediated dMyc ubiquitylation and degradation (Galletti et al., 2009; Moberg et al., 2004; Parisi et al., 2011).

Protein ubiquitylation is a reversible process in which removal of ubiquitin chains is mediated by deubiquitylating enzymes (DUBs), and the role of DUBs in controlling various cellular processes has attracted considerable interest (Clague et al., 2012; Reyes-Turcu et al., 2009). DUBs are classified into five subfamilies based on their deubiquitylating domain. Ubiquitin-specific proteases (USPs), which constitute the largest DUB subfamily, share a structurally conserved USP domain of ~350 to 450 amino acids. The USP domain is the catalytic core that mediates the cleavage of ubiquitin conjugates, whereas domains required for protein-protein interaction and substrate specificity are located within N and/or C termini of the USP protein (Komander et al., 2009; Ventii and Wilkinson, 2008). Although several ubiquitin E3 ligases have been implicated in modulating c-Myc stability, only one deubiquitylating enzyme, USP28, has been demonstrated to catalyze the deubiquitylation of Myc in mammals (Popov et al., 2007a). Thus far, no deubiquitylating enzyme has been identified that modulates dMyc function or antagonizes Ago-mediated dMyc degradation. Of the 41 predicted *Drosophila* DUBs, 21 are predicted to have a mammalian USP ortholog (Tsou et al., 2012). Interestingly, *Drosophila* does not encode an USP28 ortholog, suggesting that a distinct USP may be responsible for reversing dMyc ubiquitylation in *Drosophila*. Here, we report the identification and characterization of Puffyeye (Puf), a *Drosophila* USP that antagonizes Ago function and interacts

[1]Division of Basic Sciences, Fred Hutchinson Cancer Research Center, Seattle 98109, WA, USA. [2]Department of Genetics, Albert Einstein College of Medicine, 1300 Morris Park, Bronx 10461, NY, USA.

*Author for correspondence (eisenman@fhcrc.org)

Received 27 March 2013; Accepted 17 September 2013

Development (2013) doi:10.1242/dev.096941

genetically and physically with dMyc. We present evidence that Puf regulates dMyc activity at the level of cell and organ growth.

RESULTS

Identification of *puffyeye* (*puf, CG5794*) as a novel regulator of dMyc function

Overexpression of *dmyc* in the developing eye using three copies of *UAS-dmyc* under the control of GMR-Gal4 (denoted GMM) results in a rough eye phenotype, i.e. the adult eyes display disorganized ommatidia and are larger than wild-type eyes (Fig. 1C-D′) (Secombe et al., 2007). Previously, we described a screen to identify genes that modify the GMM-dependent eye phenotype, which led to the discovery of the histone demethylase *Little imaginal discs* (*Lid*) (Secombe et al., 2007). This screen also revealed other deficiency strains that suppress the GMM phenotype, one of which is *Df(3R)ED622*. Further analysis mapped the region to cytological band 96A13, which deletes about eight genes. Among them is *absent small or homeotic discs 2* (*ash2*), a trithorax-group gene that

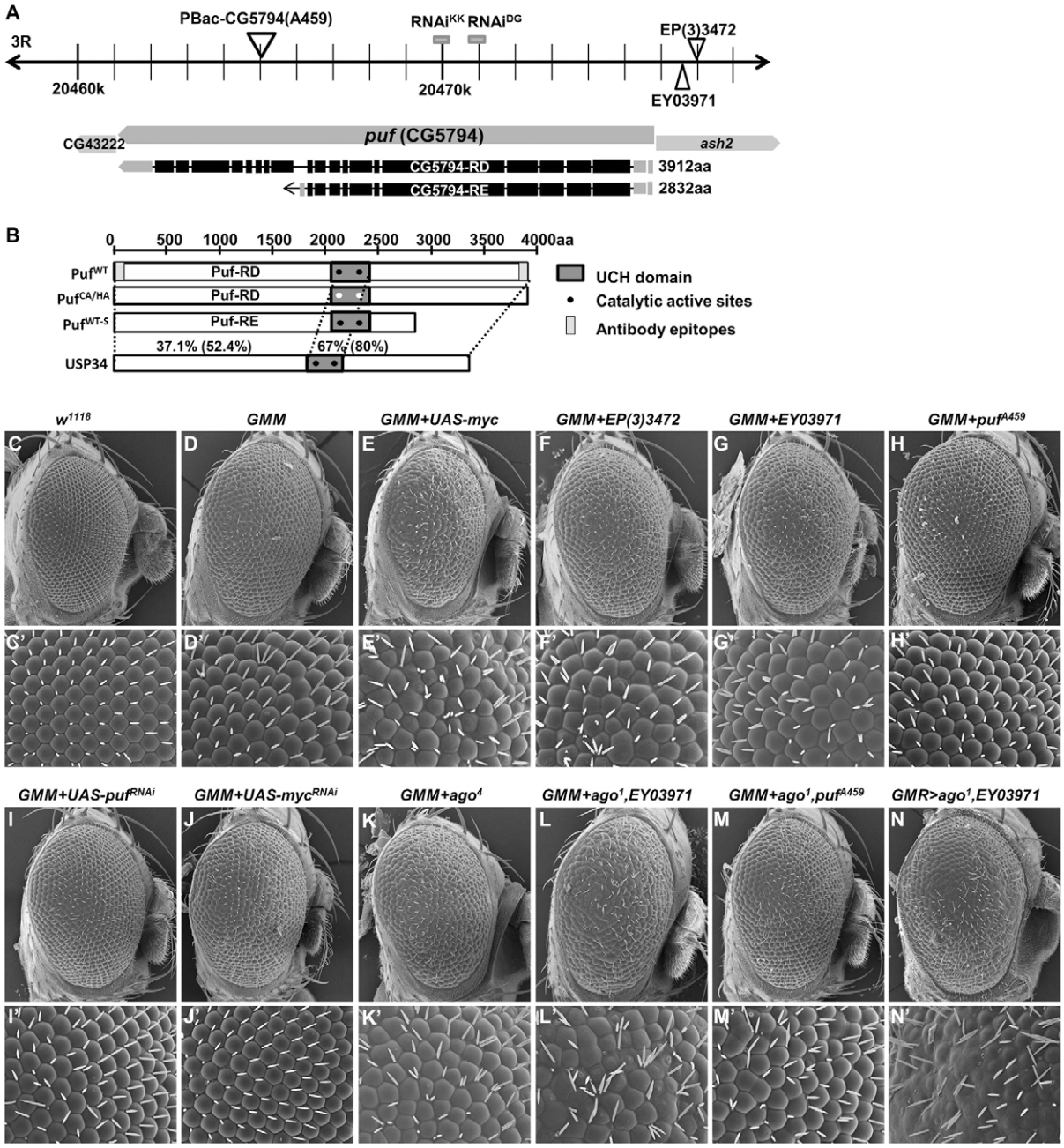

Fig. 1. *puffyeye* (CG5794) is a novel regulator of the dMyc-dependent rough eye phenotype. (A) The *puf* locus. Two of the five predicted transcript isoforms (*puf-RD* and *-RE*) are indicated (FlyBase R5.48). Coding exons are indicated as black boxes. The *puf*^{A459} insertion is situated downstream of *puf-RE*. The insertion sites of *EP(3)3472*, *EY03971* and two RNAi targeting regions are indicated. (B) Schematic of Puf^{WT}, Puf^{WT-S}, Puf$^{CA/HA}$ and USP34 proteins. Dark-grey box indicates the USP catalytic domain. Overall percentage of amino acid sequence identity and the USP domain between Puf and human USP34 are shown. Light-grey bars indicate regions used for antisera production. Black dots indicate the wild-type conserved cysteine and histidine boxes, and the white dots indicate the mutated catalytic sites. (C-N′) Scanning electron micrographs (SEMs) of the lateral view of adult compound eyes. (C-J′) SEM images show that Puf modifies GMM eye phenotype. (K-N′) SEM images show that Puf and Ago genetically interact with each other. *ago*^{1} and *ago*^{4} represent different mutant alleles. Original SEM magnification: 160× for for C-N; 750× for C′-N′.

Development (2013) doi:10.1242/dev.096941

had previously been linked to *dmyc* function (Secombe et al., 2007). As *ash2* mutants suppressed the GMM phenotype, we examined whether increased *ash2* expression could enhance the phenotype. We therefore induced the P-element insertion strains *EP(3)3472* and *EY03971* (Bellen et al., 2004; Rorth et al., 1998), both of which contain insertions within the *ash2* locus (Fig. 1A) and have the potential to induce expression of neighboring genes, including *ash2*. Interestingly, we observed enhancement of the GMM rough eye phenotype by both *EP(3)3472* and *EY03971* strains (Fig. 1F-G′). The enhanced GMM phenotype was similar to the phenotype caused by increased dMyc levels when another copy of *UAS-dmyc* was added (Fig. 1E,E′). To ascertain whether this effect was due to *ash2* expression, we generated a *UAS-ash2* transgene. However, overexpression of *UAS-ash2* had no impact on the GMM phenotype (data not shown). EP(3)3472 and EY03971 therefore enhance the GMM phenotype by inducing the expression of a gene other than *ash2*.

To identify gene(s) induced by *EP(3)3472* or *EY03971*, we performed *in situ* hybridization using antisense RNA probes against seven genes flanking these two P-element insertions. When *EP(3)3472* or *EY03971* were crossed to *apterous-Gal4* (*apGal4*), which drives expression in the dorsal compartment of the wing disc, we found that only *CG5794* expression was induced (supplementary material Fig. S1A-F; data not shown). As a positive control we showed that *ash2* was appropriately expressed when *apGal4* was crossed to *UAS-ash2* (supplementary material Fig. S1G,H). We conclude that activating *EP(3)3472* and *EY03971* induced expression of *CG5794*, but not of *ash2*. *CG5794* is an uncharacterized gene on the 3rd chromosome adjacent to *ash2*, but is transcribed in the opposite direction (Fig. 1A). *CG5794* was deleted in the deficiency strains that mapped to the cytological band 96A13, suggesting that reducing this gene contributes to the suppression of the GMM phenotype originally observed in our screen. We renamed CG5794 *puffyeye* (*puf*) to reflect its role in the dMyc-induced rough eye phenotype. Sequence comparison indicates that *puf* encodes a protein containing an ubiquitin C-terminal hydrolase 2 (UCH) domain (Fig. 1B). Several isoforms of *puf* are predicted by FlyBase, including a long (3912 amino acids, Puf^{WT}) and a short (2832 amino acids, $Puf^{WT\text{-}S}$) protein isoform (see Fig. 1A). Based on the sequence of the de-ubiquitylating domain, Puf belongs to the ubiquitin-specific protease (USP) subfamily, and is orthologous to human USP34 (Komander et al., 2009).

puffyeye is an essential gene that modifies the dMyc dependent rough eye phenotype

Using an existing *puf* mutant allele, puf^{A459}, which is generated by a *piggyBac* transposon insertion (Bellen et al., 2004), we found *puf* to be essential, with homozygous mutants dying throughout larval and pupal development. A few homozygous mutants survive to adulthood; however, they are short lived and exhibit male sterility. To verify that the lethality and adult phenotypes are caused by disruption of *puf* expression, we excised the *piggyBac* transposon. Two independent precise excision revertant alleles were recovered that were both viable and fertile with normal life spans, confirming that disruption of *puf* by the *piggyBac* transposon is responsible for the lethality and mutant phenotypes. Transcripts of both isoforms were detected by qRT-PCR in puf^{A459} animals, indicating that the *piggyBac* transposon affects translation but not transcription of *puf* (supplementary material Fig. S1I). However, puf^{A459} is unlikely to be a null mutation because the *piggyBac* is inserted in a C-terminal exon contained in the long (Puf^{WT}) isoforms and therefore will affect expression only in the long but not the short ($Puf^{WT\text{-}S}$) isoform (Fig. 1A). In addition, we obtained two RNA interference strains (RNAi, $puf\text{-}RNAi^{GD}$ and $puf\text{-}RNAi^{KK}$) that targeted all isoforms of *puf*, with no predicted off-target effects (Fig. 1A; Dickson et al., 2007). Ubiquitous knockdown with $puf\text{-}RNAi^{KK}$ using actin-Gal4 resulted in pupal lethality with no escapers when compared with the puf^{A459} mutant allele. Together, these data indicate that the puf^{A459} mutant allele is likely to be a strong hypomorph and the RNAi strains are effective in knocking down *puf* expression.

To test whether reduced *puf* levels influence the GMM phenotype in a similar manner to our original deficiency line, we crossed the GMM strain to the puf^{A459}mutant allele or the puf-RNAi strains, and found that all of these strains suppressed the GMM rough eye phenotype. The extent of GMM suppression was similar to that obtained with *dmyc*-RNAi (Fig. 1H-J′). To determine whether the genetic interaction between *puf* and dMyc is specific to Puf, rather than to a general decrease in USP function, we examined the effect on the GMM phenotype of RNAi strains against four other genes predicted to encode USP proteins (out of a total of 21 predicted USP genes): CG4165 (USP45), CG8494 (USP20), CG12082 (USP5) and CG30421 (USP43). None of these affect the GMM phenotype (data not shown), indicating that the genetic interaction between *puf* and *dmyc* is specific. To determine whether the *puf* mutation affected growth phenotypes independent of *dmyc*, we examined the effect of *puf* on the rough eye phenotype caused by *GMR-Gal4* induced overexpression of *UAS-cyclinD* and *UAS-Cdk4* (designated as GDK) (Datar et al., 2000). Varying *puf* levels did not modify the GDK rough eye phenotype (supplementary material Fig. S2A-E). Taken together, our data indicate that *puf* specifically modifies dMyc dependent growth in the eye.

Antagonism between *puf* and *ago*

Because *puf* is predicted to encode a deubiquitylating enzyme, and was identified as a regulator of dMyc-mediated cell growth, we asked whether *puf* antagonizes the dMyc ubiquitin ligase *archipelago* (*ago*). Consistent with its role in regulating dMyc levels, flies with null mutations of *ago* have elevated levels of dMyc due to stabilization of the dMyc protein (Moberg et al., 2004). Although *ago* heterozygotes alone did not display any eye phenotype, they strongly enhanced the GMM rough eye phenotype (Fig. 1K,K′). Enhancement of the GMM phenotype caused by reducing *ago* gene dose was further augmented when Puf expression was increased using the P-element insertion strains *EP(3)3472* or *EY03971* (Fig. 1L,L′). Conversely, this phenotype was mildly suppressed by reduced Puf levels (Fig. 1M,M′). These findings demonstrate that *puf* and *ago* act antagonistically to regulate dMyc function in the eye.

Puf promotes growth in the eye

Based on its predicted ability to regulate dMyc stability, we examined in greater detail the ability of Puf to promote cell growth. Overexpressing Puf in the eye using *EP(3)3472* or *EY03971* caused a mild rough eye phenotype with increased ommatidial size when compared with the control, an effect similar to that caused by dMyc overexpression (Fig. 2A-C′). This rough eye phenotype was suppressed when *puf* levels were reduced by loss of one *puf* allele or RNAi knockdown (Fig. 2D-E′), consistent with the ability of *EP(3)3472* or *EY03971* to induce *puf* expression. Importantly, the Puf eye phenotype was modified by altering dMyc levels (Fig. 2F-G′), suggesting that misregulation of dMyc is an essential contributor to the Puf-induced phenotype. We also noted that Puf overexpression (resulting from GMR driven expression of *EY03971*) in the context of the *ago* heterozygous mutant produced a very

Development (2013) doi:10.1242/dev.096941

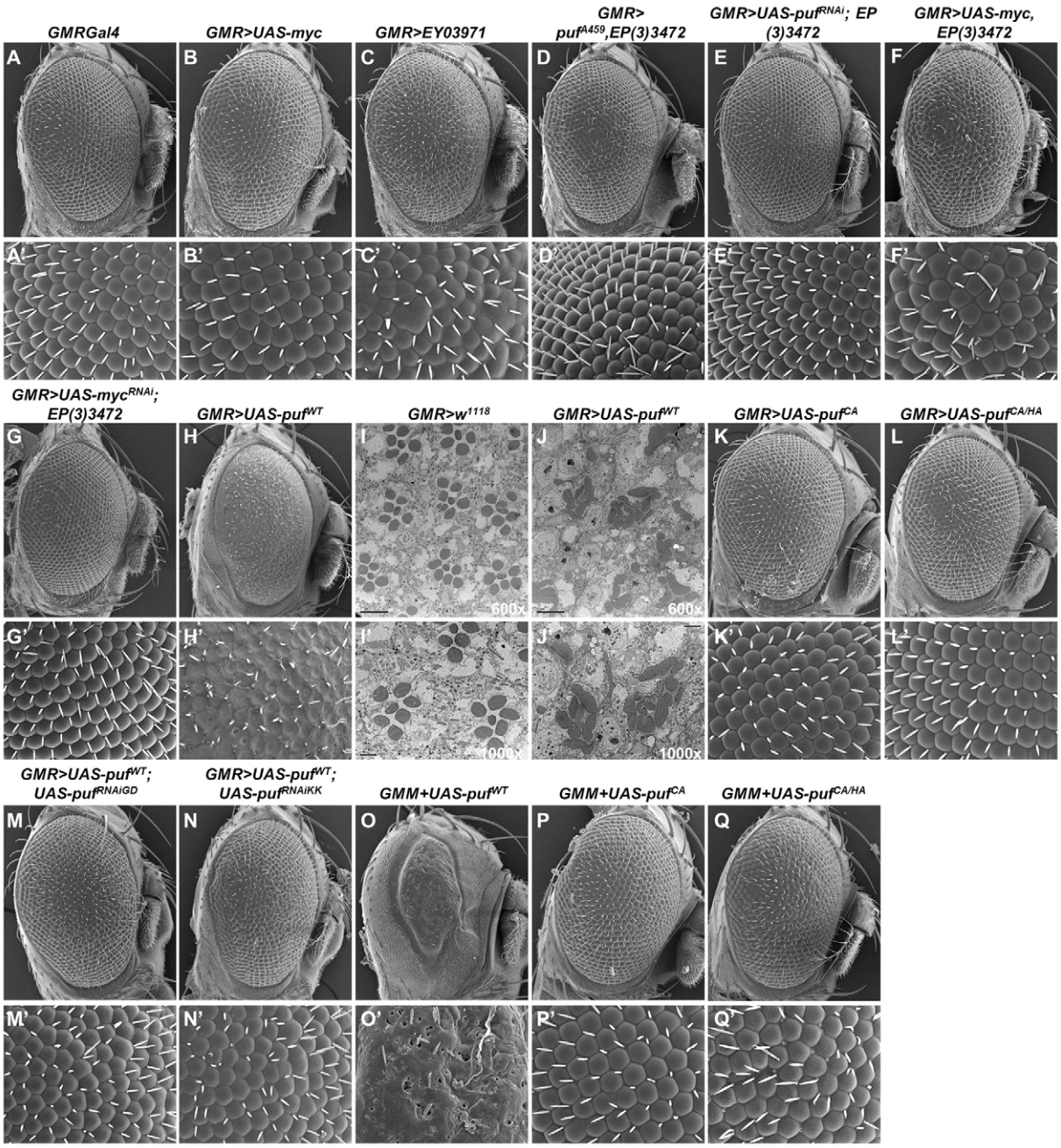

Fig. 2. Puf promotes growth in the eye in a dMyc-dependent manner. (A-C′) Lateral view of scanning electron micrographs (SEMs) show eye phenotypes caused by dMyc or Puf activation. (D-G′) SEM shows dMyc and Puf genetically interact to modify eye phenotype. (H,H′,K-N′) SEM shows eye phenotype of *UAS-puf* transgenes. (I-J′) Transmission electron micrographs (TEM) show ommatidia of adult compound eyes. (O-Q′) SEM shows modification of GMM eye phenotype by *UAS-puf* transgenes. Original SEM magnification: 160× for A-H,K-Q; 750× for A′-H′,K′-Q′. Original TEM magnification: 600× for I,J; 1000× for I′,J′.

strong rough eye phenotype even in the absence of dMyc overexpression (Fig. 1N), consistent with the notion that Ago antagonizes Puf function. This may be due to an effect of Puf on endogenous dMyc, as well as on other proteins important for eye development, such as CycE (Secombe et al., 1998) (see Discussion).

To analyze the role of Puf in greater detail, we generated *UAS-puf* transgenic flies and antisera against either the N-terminal (anti-PufN) or the C-terminal region (anti-PufC) of Puf. To date, five mRNA isoforms of *puf* have been described, all of which are predicted to contain identical N-terminal regions and the conserved core deubiquitylating domain of ~400 amino acids, but differ in their C-terminal regions (Fig. 1A,B) (Tweedie et al., 2009). Protein domains outside of the core deubiquitylating domain may be important for substrate recognition and protein-protein interaction, suggesting the possibility that the long and short isoforms of Puf might possess different activities. We therefore generated *UAS-puf* transgenic flies for both isoforms. Transgenic flies containing the wild-type Puf-RD long-isoform cDNA encoding a protein of 3912 amino acids are designated as *UAS-puf*^{WT}, whereas flies containing the Puf-RE short-isoform cDNA encoding a 2832 amino acid protein are designated as *UAS-puf*$^{WT\text{-}S}$ (Fig. 1B). To determine the functional relevance of its enzymatic activity, we carried out site directed mutagenesis to mutate conserved critical residues within the UCH catalytic domain (Komander et al., 2009). We generated

Development (2013) doi:10.1242/dev.096941

transgenic flies containing either (1) a single mutation in the conserved cysteine box by replacing the catalytic cysteine (Cys2024) with alanine, designated *UAS-puf*^{CA}; or (2) triple mutations in which the cysteine box mutation was combined with alanine substitutions of histidine (His2974) and asparagine (Asp2302) within the histidine box, designated *UAS-puf*$^{CA/HA}$ (Fig. 1B). The transgenic flies containing cDNA of triple mutations for the short isoform are designated *UAS-puf*$^{CA/HA\text{-}S}$.

As expected, *GMR-Gal4 >UAS-puf*^{WT} expressed considerably higher levels of Puf protein (supplementary material Fig. S1J), and resulted in a more pronounced rough eye phenotype than *EP(3)3472* or *EY03971*. The *UAS-puf*^{WT} phenotype was stronger than that observed following overexpression of dMyc (Fig. 2A,B,H), suggesting that Puf affects targets in addition to dMyc. A similar phenotype was observed when the short isoform, *UAS-puf*$^{WT\text{-}S}$, was overexpressed (supplementary material Fig. S2F). Adult eyes overexpressing Puf using *UAS-puf*^{WT} displayed marked disorganization of the ommatidia compared with control (Fig. 2I,J). This phenotype was strongly suppressed following RNAi knockdown of Puf, further confirming that the *puf* encoding transgene is responsible for the rough eye effect (Fig. 2M,N).

In contrast to our findings with wild-type Puf, overexpression of enzymatic mutant *puf*^{CA}, *puf*$^{CA/HA}$ or the short isoform *puf*$^{CA/HA\text{-}S}$ failed to elicit any detectable eye phenotype (Fig. 2K,L; supplementary material Fig. S2G), despite being expressed at similar levels (supplementary material Fig. S4A), indicating that the rough eye phenotype caused by wild-type Puf depends on its deubiquitylating activity. Our data also show that a single mutation in the cysteine box of the catalytic domain is as efficient in inactivating Puf activity as triple mutations in both the cysteine and histidine boxes. Furthermore, we demonstrate that expression of *puf*^{WT} or *puf*$^{WT\text{-}S}$ strongly enhances the GMM eye phenotype by causing massive cell death, as indicated by the extreme disorganization of ommatidia and reduction in overall size of the eye (Fig. 2O; supplementary material Fig. S2H). As expected, expression of Puf-containing catalytic domain mutations did not modify the GMM eye phenotype (Fig. 2P,Q; supplementary material Fig. S2I).

Puf is necessary for wing growth

Because different tissues have been reported to exhibit differences in growth regulation (Herranz and Milán, 2008), we next examined wing development to determine whether the strong interaction between *puf* and *dmyc* can be detected in organs other than the eye. We used the *BxΔK-Gal4* driver to overexpress *UAS-dmyc* in the dorsal part of the larval wing disc that gives rise to the upper layer of adult wing bilayer. As shown in Fig. 3A,B, this caused the adult wing to curve downwards when compared with the straight wing of the control. Such a downward curving wing is indicative of increased cell size in the dorsal layer relative to the ventral layer, as previously observed for other genes known to promote cell growth (Montagne et al., 1999). Similarly, *BxΔK-Gal4* driven *puf* expression through either *EP(3)3472* or *EY03971* displayed the same downward curved wing phenotype, suggesting that *puf* overexpression also increased cell size (Fig. 3C,D). Furthermore increased Puf expression enhanced the downward wing curvature caused by dMyc overexpression (Fig. 3E,F), consistent with the genetic interaction we observed between *puf* and *dmyc* in the eye (Fig. 2). Conversely, when levels of either dMyc or Puf were reduced by RNAi knockdown, the wing exhibited upward curvature, indicating that cells on the dorsal side are now smaller relative to their ventral counterparts (Fig. 3G,H).

The expression of high levels of either wild-type Puf isoform caused a much stronger wing phenotype, whereas no wing phenotype was detected following expression of the catalytic Puf^{CA}, Puf$^{CA/HA}$ and Puf$^{CA/HA\text{-}S}$ (supplementary material Fig. S3A-F). The severe wing phenotype observed with the wild-type isoforms resulted from extensive cell death, as evidenced by increased cleaved caspase 3 staining (supplementary material Fig. S3G-J). The increased cell death phenotype was partially suppressed when *UAS-puf*^{WT} was co-expressed with *UAS-Diap*, an inhibitor of apoptosis (data not shown) (Orme and Meier, 2009; Steller, 2008), suggesting that Puf also plays a role in the apoptotic pathway. As reported in previous studies, we also observed that dMyc induced apoptosis in a dose-dependent manner in the wing discs. However Puf overexpression has a stronger effect in inducing apoptosis than dMyc. For example, when Puf is overexpressed using *BxΔK*-Gal4 and *engrailed*-Gal4, it caused cell death, whereas when dMyc was induced with the same Gal4 drivers, no apoptosis was observed. This suggests that apoptosis due to Puf is largely independent of dMyc, a notion that is consistent with previous studies indicating that Myc-induced apoptosis is highly context dependent (Montero et al., 2008).

To further explore interaction between dMyc, Puf and Ago, we used *engrailed*-Gal4 (*enGal4*) to drive their expression in the posterior compartment of the wing disc. dMyc overexpression, or reduction of *ago* activity, using an *ago* RNAi knockdown transgene, significantly increased the area of the posterior compartment, as well as the ratio between the posterior and anterior areas, owing to enlarged cell size (Fig. 3I-K,Q; supplementary material Fig. S3K-M) (Flockhart et al., 2006; Johnston et al., 1999; Moberg et al., 2004). The effect of dMyc overexpression was mitigated by increasing Ago levels (Fig. 3L,Q). Conversely, reducing dMyc or Puf levels via RNAi knockdown caused reduction of the posterior region (Fig. 3M-O,Q). This was due to decreased cell size and not to apoptosis, as indicated by the increased density of bristles and an absence of cleaved caspase 3 staining (supplementary material Fig. S3N-O; data not shown). *puf* RNAi knockdown partially suppressed the size increase caused by dMyc overexpression in the posterior compartment (Fig. 3P,Q; supplementary material Fig. S3P). Interestingly, this combination caused a mild wing vein phenotype, which was also observed after *puf* and *ago* RNAi knockdown (Fig. 3K,N,P), suggesting the existence of other Puf and Ago substrates in the wing because no vein phenotype was observed in dMyc overexpression or knockdown (Fig. 3J,O).

Post-transcriptional regulation of dMyc abundance by Puf

Because Puf is predicted to be a deubiquitylating enzyme, we determined whether Puf influences dMyc protein abundance by altering dMyc stability. We examined dMyc levels in wing imaginal discs of wild-type control (*w*^{1118}) or the *puf*^{A459} hypomorphic mutant. Western blots of protein lysates from wing disc cells show that endogenous dMyc protein levels are reduced in *puf*^{A459} mutant cells relative to wild-type cells (*w*^{1118}), whereas *dMyc* transcript levels were not significantly changed (Fig. 4A; supplementary material Fig. S1I). Moreover, dMyc levels increased when *UAS-puf*^{WT} is overexpressed, whereas dMyc is unaffected by *UAS-puf*$^{CA/HA}$ overexpression (Fig. 4B). Immunostaining of wild-type wing discs show that endogenous dMyc is widely expressed, with highest levels in the wing pouch and the notum, as previously reported (Galletti et al., 2009; Wu and Johnston, 2010). Endogenous Puf, by contrast, is ubiquitously expressed at low levels without any evident pattern (Fig. 4C,C′). Widespread overexpression of *UAS-dMyc* in the wing pouch using the *rnGal4* driver does not alter Puf levels or expression pattern, indicating that dMyc does not regulate Puf protein levels (Fig. 4D,D′).

Development (2013) doi:10.1242/dev.096941

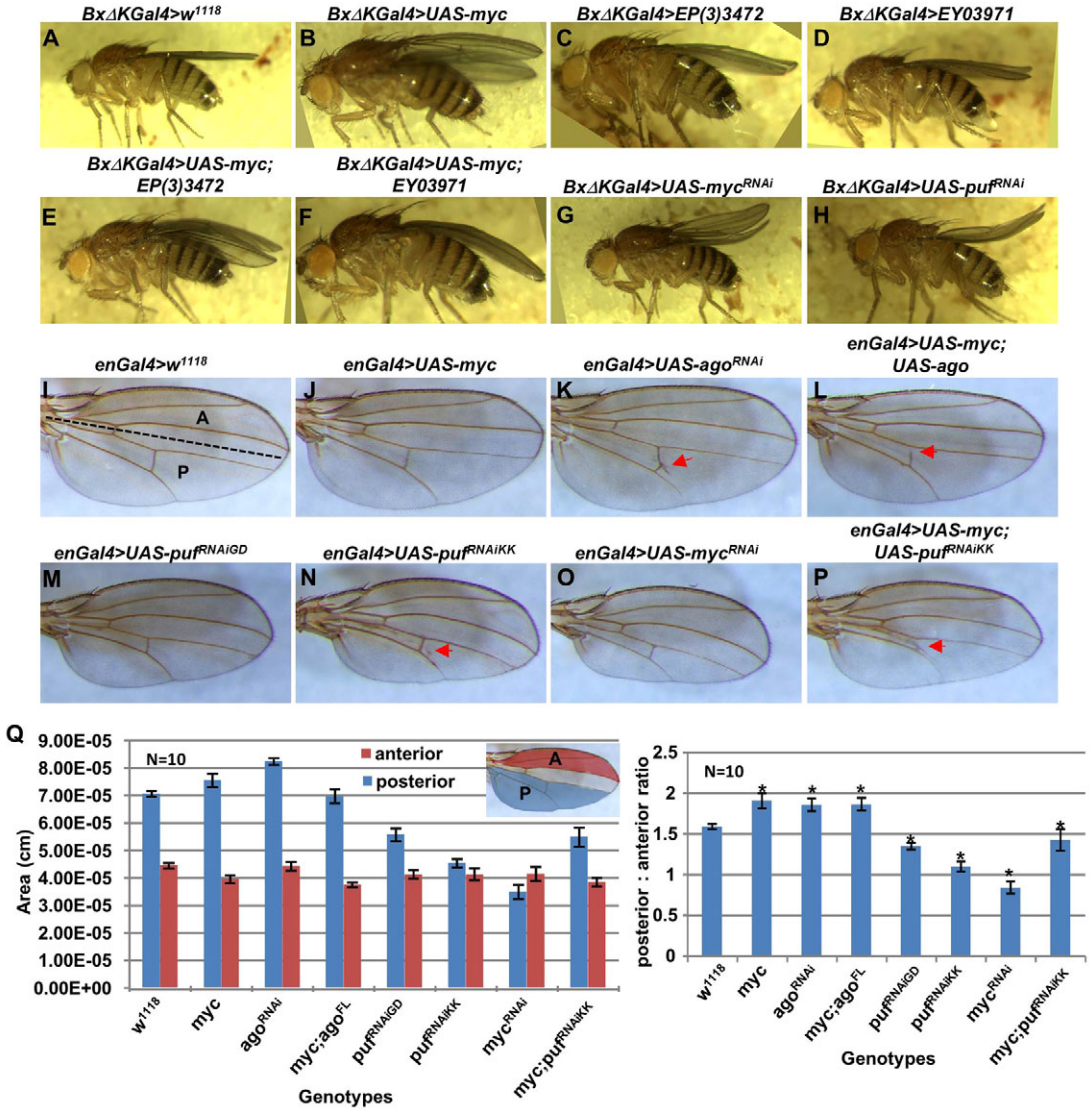

Fig. 3. Puf is necessary for growth in the wing. (A-H) Wing phenotypes caused by BxΔK-Gal4-driven transgene expression in the dorsal compartment of the wing. (I-P) Wing phenotypes caused by *en-Gal4*-induced transgene expression in the posterior compartment of the wing. Dashed line in I indicates the anterior-posterior boundary. Arrows indicate vein phenotype. (Q) Quantification of the areas of anterior and posterior compartments of the adult wing (left panel) and the ratio of posterior:anterior compartments (right panel). Anterior (red) and posterior (blue) areas were measured using ImageJ software (10 wings per genotype). Error bars indicate s.e.m. **P*<0.001, Student's *t*-test.

However, when *UAS-puf*^{WT} is overexpressed using *rnGal4*, dMyc levels are markedly upregulated in domains overexpressing Puf (Fig. 4E,E′). Similarly, *UAS-puf*^{WT} expression driven by *dppGal4* resulted in elevated dMyc levels in *dpp*-expressing domains. Importantly, expression of catalytic mutant *puf*$^{CA/HA}$ had no effect on dMyc (Fig. 4F-H′). In western blots, the elevation of dMyc levels by *puf*^{WT} is even more apparent when dMyc and Puf^{WT} are co-overexpressed, whereas this effect is not observed when either Puf^{CA} or Puf$^{CA/HA}$ are co-expressed with dMyc (Fig. 4I,J). Overexpression of wild-type and mutant forms of Puf$^{WT\text{-}S}$, the short isoform of Puf, gave the same results as with full-length Puf (supplementary material Fig. S4A,B). Therefore, the ability of both isoforms of Puf to regulate dMyc levels requires a wild-type catalytic deubiquitylation domain. The effect of Puf on dMyc levels is not limited to mitotic tissue as Puf also regulates dMyc levels in fatbody, a larval tissue.

To determine whether Puf regulates dMyc levels by increasing dMyc stability, we performed chase experiments using wing discs from late 3rd instar larvae treated with the protein synthesis inhibitor cycloheximide. In control wing discs, endogenous dMyc protein levels dropped to ~50% of untreated control levels by 30 minutes after cycloheximide addition, and was barely detectable after a 2-hour chase (Fig. 5A,B). This rate of dMyc degradation is unchanged by overexpression of catalytic domain mutant Puf$^{CA/HA}$ (Fig. 5A,B). By contrast, when Puf^{WT} is overexpressed, dMyc abundance remained at 60% of initial levels following 2 hours of treatment with cycloheximide (Fig. 5A,B). We observed very similar effects when Puf was co-overexpressed with dMyc (Fig. 5C). We also performed qRT-PCR to determine whether Puf controls dMyc abundance at the transcriptional level. No change in *dMyc* transcript levels was observed in wing discs overexpressing Puf^{WT} (Fig. 5D). Together, these results are consistent with the notion that Puf deubiquitylating activity antagonizes Ago to regulate dMyc protein stability.

Interactions between dMyc, Puf and Ago proteins

To determine whether Puf regulates dMyc directly, we asked whether these proteins are localized to the same subcellular

Development (2013) doi:10.1242/dev.096941

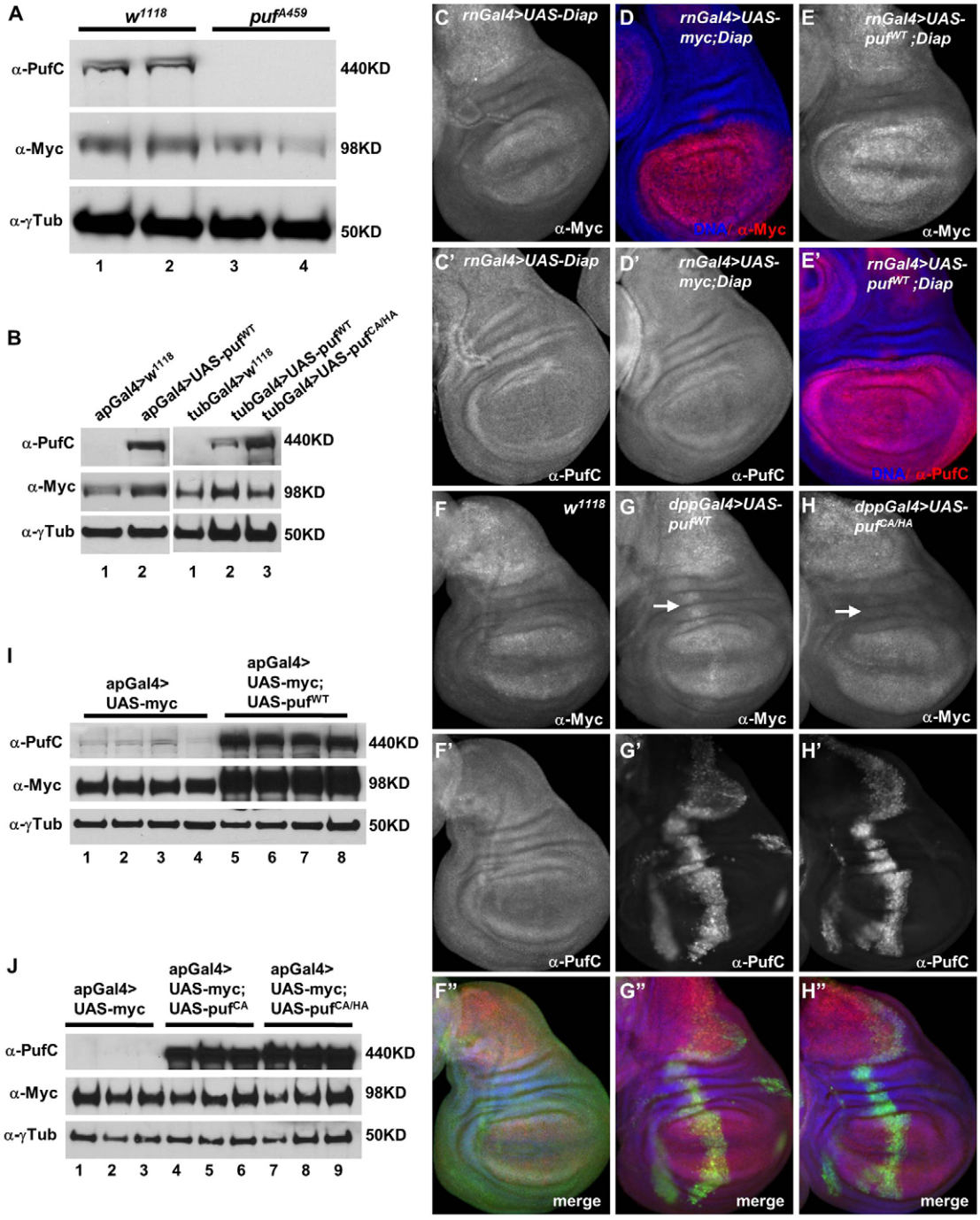

Fig. 4. Puf regulates dMyc levels in a deubiquitylating activity-dependent manner. (A,B) Western blots of protein lysates from 3rd instar larval wing discs. (A) w^{1118} wild-type control (lanes 1, 2) and puf^{A459} homozygous mutant (lanes 3, 4). Each lane used protein lysates from 20 wing discs. γ-Tubulin served as loading control. (B) Effect of Puf ^{WT} and catalytic mutants on endogenous dMyc levels. Each lane used protein lysates from 10 wing discs. (C-H″) Immunostaining of 3rd instar larval wing disc showing effect of Puf on dMyc levels. (I,J) Effect of Puf ^{WT} and catalytic mutants on overexpressed dMyc protein levels. Each lane used protein lysates from 10 wing discs after a 20-hour induction.

compartment *in vivo* and associate in a protein complex. dMyc functions as a transcription factor and is predominantly localized in the nucleus; however, Puf lacks a conventional nuclear localization signal. We examined Puf localization using anti-PufC in immunostaining experiments. Employing antisera against the nuclear envelope structural protein lamin C (Riemer et al., 1995) to demarcate nuclei, we found that endogenous Puf localizes within the lamin C-marked nuclear regions (Fig. 6A). In addition, we find that both Puf isoforms are nuclear localized, as is dMyc (Fig. 6B; data not shown).

To examine whether Puf and dMyc proteins interact, we performed co-immunoprecipitation experiments using protein lysates from wing discs co-expressing dMyc and Puf^{WT} or $Puf^{CA/HA}$. We first used anti-PufC to immunoprecipitate Puf and then carried out immunoblotting of the precipitate with anti-dMyc. The results show that dMyc is present in anti-Puf^{WT} immunoprecipitates

Development (2013) doi:10.1242/dev.096941

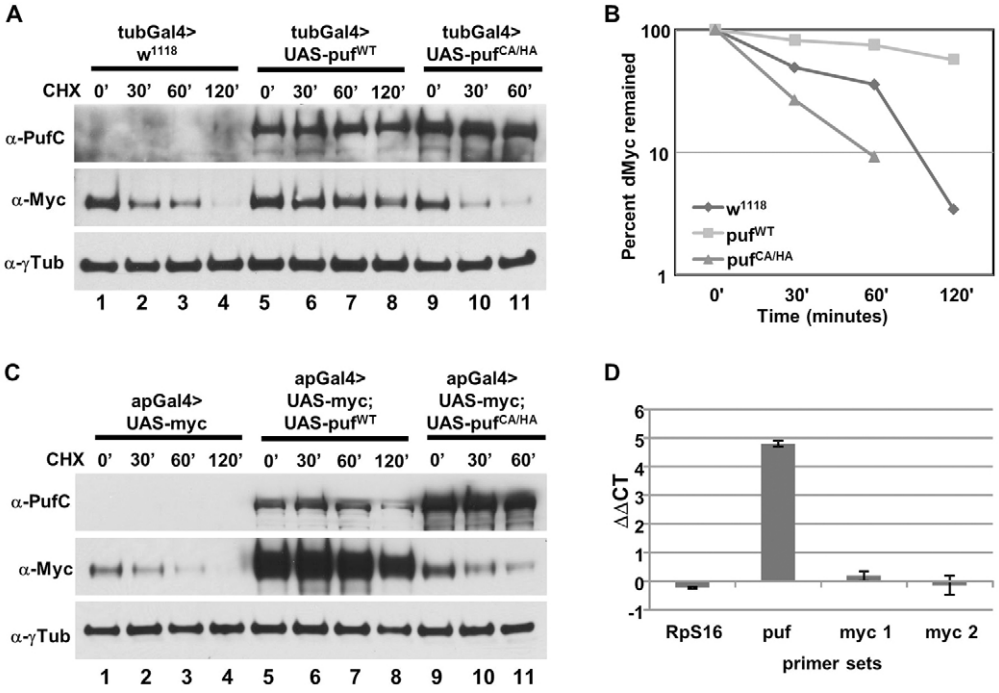

Fig. 5. Post-translational regulation of dMyc abundance by Puf. (A) Endogenous dMyc levels at increasing times following treatment with cycloheximide (CHX chase) to determine the stability of dMyc in control wing disc cells (lanes 1-4) or in cells overexpressing Puf^{WT} (lanes 5-8) or Puf$^{CA/HA}$ (lanes 9-11). Protein lysates were isolated from 12 wing discs at the indicated time points after CHX treatment. (B) The quantification of dMyc levels after the addition of CHX. The amount of dMyc remaining was obtained by normalizing signals generated by mouse monoclonal dMyc antibody to that of γ-tubulin using ImageJ software. Time zero was set at 100%. The data are plotted as percentages of dMyc remaining over time zero for each point. (C) Stability of overexpressed dMyc measured in CHX-chase experiments. Protein lysates from wing discs overexpressing dMyc (lanes 1-4), dMyc+ Puf^{WT} (lanes 5-8) or dMyc+Puf$^{CA/HA}$ (lanes 9-11). (D) qRT-PCR determination of relative levels of *dMyc* mRNA following overexpression of Puf (*tub-Gal4, UAS-puf^{WT}*). Relative expression levels (ΔΔCT) were calculated using *RpS16* as internal control. Data represent mean of three biological samples analyzed in duplicate. Error bars indicate s.e.m. Transgenes were induced for 20 hours using temperature-inducible Gal4 drivers.

(Fig. 6C). Precipitates with pre-immune serum showed only a low intensity background band. Importantly, the ability of Puf to form a protein complex with dMyc is independent of its deubiquitylating function as Puf$^{CA/HA}$ also co-immunoprecipitated with dMyc (Fig. 6C). Although expressed at much lower levels, endogenous dMyc was detected with anti-PufC, but not with pre-immune sera in wing discs expressing either Puf^{WT} or Puf$^{CA/HA}$ (Fig. 6D). To further verify the interaction between Puf and dMyc, we performed immunoprecipitation using anti-sera against dMyc and immunoblotted with anti-Puf. Both Puf^{WT} and Puf$^{CA/HA}$ co-immunoprecipitated with dMyc, albeit with somewhat lower efficiency than in anti-Puf immunoprecipitates (supplementary material Fig. S5A). These data suggest that mutations in the Puf catalytic domain do not impair its ability to interact with dMyc.

Previous studies have demonstrated that some deubiquitylating enzymes associate with multiple proteins in addition to their substrates, including their antagonistic E3 ligases (Brooks et al., 2007; Hu et al., 2006; Sheng et al., 2006; Sowa et al., 2009; Ventii and Wilkinson, 2008). We therefore asked whether Puf co-immunoprecipitates with Ago. Because endogenous levels of Ago are extremely low, we used wing discs co-overexpressing Ago as well as Puf. We found that anti-PufC immunoprecipitates an Ago-specific protein band, and that dMyc is also present in these immunoprecipitates (Fig. 6E), indicating that Ago interacts with both Puf and dMyc. The apparent molecular weight difference between the Ago proteins detected in the input and the anti-Puf lanes prompted us to investigate the specificity of Ago antisera. We found endogenous Ago is present as two differentially migrating bands that are both reduced when Ago is knocked down by *ago* RNAi, and increased by Puf^{WT} overexpression (Fig. 6F). Overexpressed *UAS-ago* predominantly results in the upregulation of the higher molecular weight bands (Fig. 6F). This raises the possibility that a modified subset of Ago protein is present in the complex with Puf. Although our data does not allow us to conclude that dMyc, Ago and Puf are present in a single complex, as was reported for USP28, Myc and Fbw7 (Popov et al., 2007b), it suggests close interaction among these components of the ubiquitin machinery and their dMyc substrate.

Puf regulates Ago and Cyclin E

Several ubiquitin ligases have been shown to be regulated post-translationally by ubiquitylation and deubiquitylation (de Bie and Ciechanover, 2011). Recently, Fbw7 was reported to be auto-ubiquitylated in a phosphorylation- and substrate-dependent manner (Min et al., 2012). To examine whether Puf affects Ago levels, we carried out immunostaining experiments demonstrating that endogenous Ago is expressed throughout the larval wing disc (Fig. 7A). Overexpressing either isoform of wild-type Puf (Puf^{WT} or Puf$^{WT\text{-}S}$) in either the dorsal or the anterior compartment of the wing disc using a temperature-inducible *ap-Gal4,tub-Gal80^{ts}* or *ci-Gal4,tub-Gal80^{ts}* driver results in higher levels of Ago (Fig. 7B; supplementary material Fig. S6B; Fig. S7B), whereas overexpressing the catalytically inactive Puf (Puf$^{CA/HA}$ or Puf$^{CA/HA\text{-}S}$) does not affect Ago (Fig. 7C; supplementary material Fig. S6C; Fig. S7C). This result was confirmed by an immunoblot from late 3rd instar larval wing discs overexpressing Ago, showing overexpressed Puf^{WT}, but

Development (2013) doi:10.1242/dev.096941

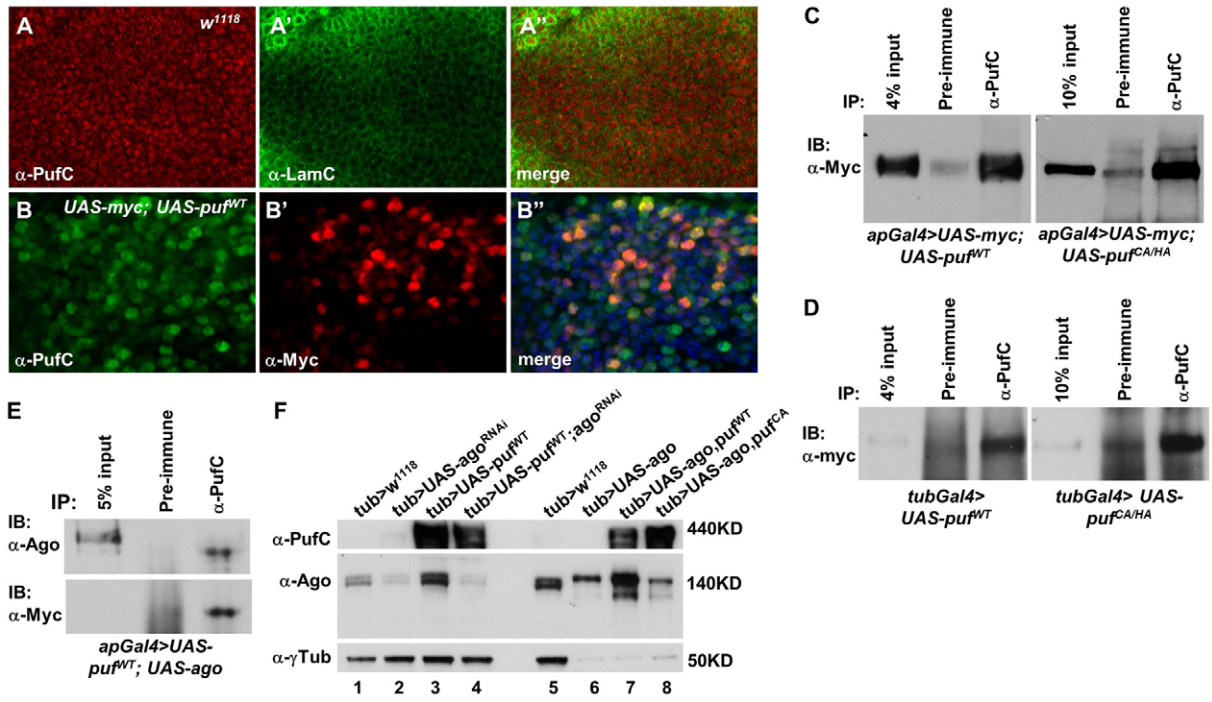

Fig. 6. Puf is a nuclear protein and interacts with dMyc and Ago. (A-A") Immunostaining of the 3rd instar larval wing disc of w^{1118} stained with anti-Puf (red, A) and anti-lamin C (A′, green) showing nuclear localization of endogenous Puf. (A") Merge of A and A'. (B-B") Immunostaining of the 3rd instar larval wing disc expressing *UAS-dMyc, UAS-puf*^{WT} stained with anti-dMyc (red, B′) and anti-Puf (B, green) showing colocalization of Puf and dMyc in the nucleus. (B") Merge of B and B'. (C) Co-immunoprecipitation showing that both Puf^{WT} (left panel) and Puf$^{CA/HA}$ (right panel) form a protein complex with dMyc. (D) Co-immunoprecipitation showing endogenous dMyc forms a complex with Puf^{WT} or Puf$^{CA/HA}$. (E) Co-immunoprecipitation showing Puf forms protein complexes with Ago or dMyc. All co-immunoprecipitations were carried out using protein lysates isolated from 3rd instar larval wing discs of indicated genotypes, immunoprecipitated with pre-immune or anti-Puf antisera, and analyzed by western blot using appropriate antisera. Transgenes were induced for 20 hours using temperature-inducible Gal4 drivers. (F) Western blot showing specificity of anti-Ago and effect of Puf on endogenous Ago (lanes 1-5; 30 discs/lane) and overexpressed Ago (lanes 6-8; 10 discs/lane).

not the catalytic mutant Puf^{CA}, increased Ago levels (Fig. 6F). Furthermore, downregulation of Puf using an RNAi transgene mildly reduces endogenous Ago levels (Fig. 7D; supplementary material Fig. S7D). The physical interaction between Puf and Ago, and the requirement for Puf and its functional deubiquitylase domain in the regulation of Ago expression suggests that Ago is likely to be a substrate of Puf. Conversely, although RNAi knockdown of *Ago* in the dorsal wing disc compartment resulted in elevated levels of the known Ago substrate dMyc, it did not elevate endogenous Puf levels, suggesting Puf itself is not an Ago substrate (supplementary material Fig. S6F,K,L; Fig. S7K,L).

Because Ago in *Drosophila* and Fbw7 in mammalian cells have been shown to promote protein turnover of CycE (Koepp et al., 2001; Moberg et al., 2001), we asked whether Puf is also involved in CycE regulation. Western blots of protein lysates from wing discs overexpressing wild-type Puf showed markedly increased levels of overexpressed CycE, whereas overexpression of the deubiquitylation domain mutant Puf^{CA} had no effect on CycE abundance (Fig. 7H). Furthermore, cycloheximide chase experiments using wing discs from late 3rd instar larvae show that high levels of CycE are maintained in wing discs overexpressing CycE and Puf^{WT} after 6 hours of cycloheximide treatment. By contrast, CycE levels were strongly reduced in wing discs overexpressing CycE alone or co-overexpressed with mutated Puf^{CA} (Fig. 7I), indicating that Puf regulates CycE levels by increasing its stability dependent on a wild-type deubiquitylation domain. qRT-PCR confirms that Puf has no significant effect on the transcript levels of *ago* or *cycE* (supplementary material Fig. S6M).

Interestingly, Ago levels are also elevated when dMyc is overexpressed, and reduced when dMyc was knocked down (Fig. 7E,F; supplementary material Fig. S7E,H). Importantly, the upregulation of Ago by overexpressed Puf is not solely a consequence of dMyc upregulation as Puf^{WT} overexpression induces Ago when dMyc is simultaneously knocked down (Fig. 7G; supplementary material Fig. S6D,I,J; Fig. S7G-J). Because we failed to observe a significant increase in *ago* RNA expression upon dMyc overexpression (supplementary material Fig. S6N), we surmise that the induction of Ago by dMyc is indirect, possibly as a result of the effect of dMyc on cell growth and mitochondrial function (Mandal et al., 2010). Taken together, our data suggest that negative autoregulation of dMyc can be mediated through dMyc induction of Ago, and Puf plays an important role in modulating dMyc, CycE and Ago functions by regulating their protein levels (summarized in Fig. 7J).

DISCUSSION

Ubiquitin ligases act as key components of the ubiquitin machinery by specifically ubiquitylating protein substrates to mark them for proteasome-mediated destruction (Varshavsky, 2012). Importantly, protein ubiquitylation is reversible through the activity of deubiquitylating enzymes (DUBs), which act to maintain a dynamic balance of ubiquitylated substrates and to control ubiquitin-dependent signaling pathways (Clague et al., 2012; Ventii and Wilkinson, 2008). Systematic RNAi knockdowns in *Drosophila* demonstrated that most DUBs have non-redundant functions (Tsou et al., 2012). In this report, we describe a novel DUB that regulates Myc and CycE protein stability in *Drosophila*.

Development (2013) doi:10.1242/dev.096941

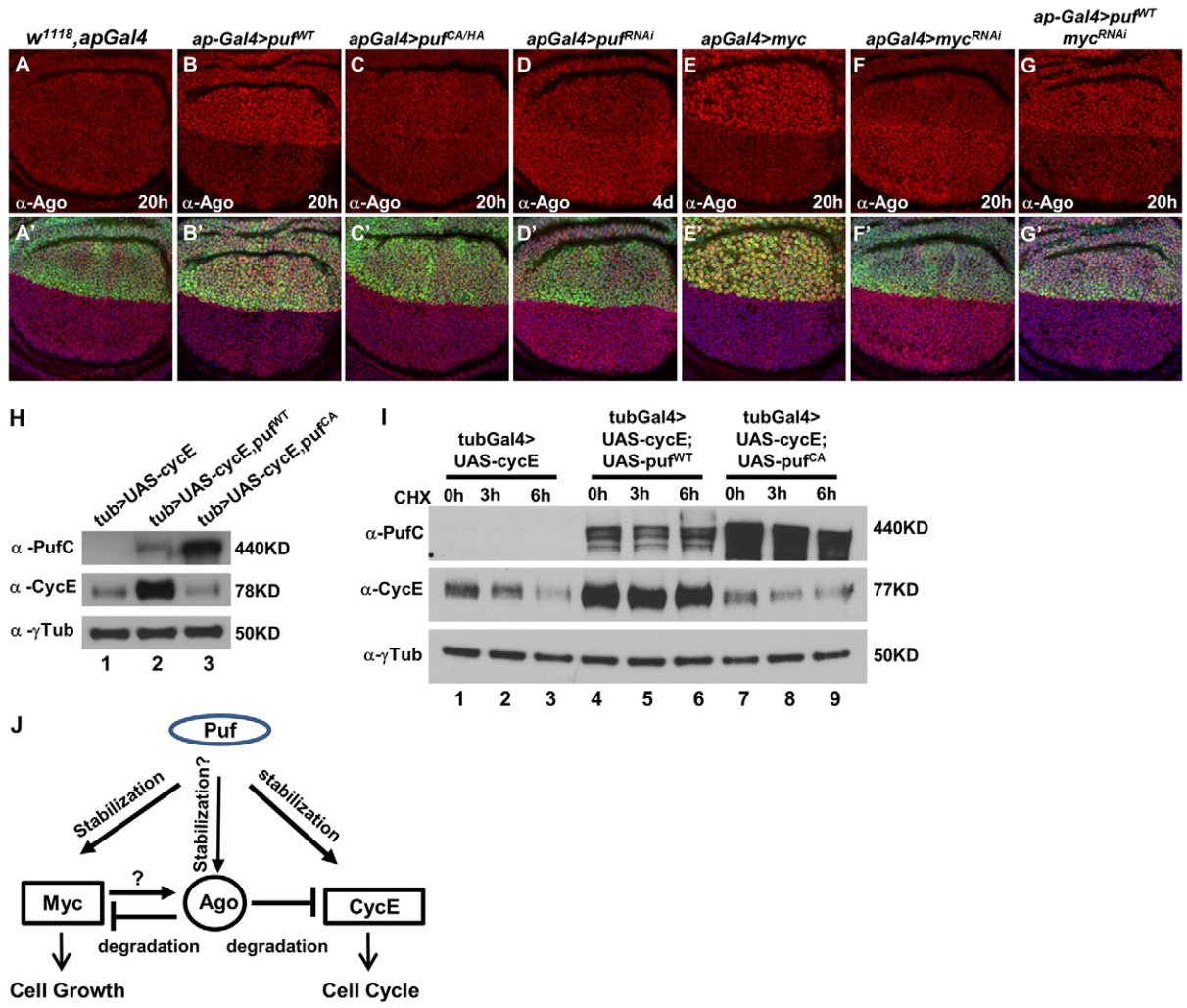

Fig. 7. Post-translational regulation of Ago and CycE levels by Puf. (A-G') Immunostaining of the 3rd instar larval wing disc showing that Puf and dMyc regulate Ago levels. All transgene expression was marked by GFP, induction time is indicated. (H) Western blot using anti-CycE showing effect of Puf on CycE levels. (I) CHX chase experiments for overexpressed CycE alone (lanes 1-3), CycE+ Puf^{WT} (lanes 4-6) or CycE+ Puf^{CA} (lanes 7-9). Fifteen discs per time point. (J) The complex regulatory loop among Puf, Myc and Ago.

Although a great deal has been learned recently concerning ubiquitin ligases that interact with Myc proteins (Müller and Eilers, 2009), to date only one DUB has been reported that targets Myc (Popov et al., 2007b). Here, we have employed a genetic screen based on the rough eye phenotype induced by dMyc overexpression in the eye (GMM) in *Drosophila*. This screen led to the identification of a USP-type DUB, which we have named Puffyeye (Puf; CG9754), as a novel regulator of dMyc function *in vivo*. We found that reduced *puf* expression suppresses, whereas *puf* overexpression augments, the GMM phenotype. This phenotype is largely an effect of cell overgrowth (Secombe et al., 2007), yet overgrowth in the eye due to cyclin D/Cdk4 was not influenced by altered Puf abundance. Moreover, knockdown of four other USPs had no effect on the GMM phenotype. This suggests that *puf* possesses specificity for dMyc-induced growth in the eye. Indeed, *puf* itself induced a dose-dependent rough eye phenotype, displaying augmented ommatidial size that can be modulated by altering dMyc levels. In the wing disc, dMyc and Puf also were found to collaborate in cell growth. We also found that Puf is essential for normal development, consistent with a crucial role for Puf in cell growth.

dMyc levels markedly increase in cells in which *puf* is overexpressed, whereas dMyc levels are decreased in Puf hypomorphic mutants. We show that these changes in dMyc are predominantly post-translational. This is consistent with our finding that Puf overexpression results in a dramatic increase in dMyc protein stability. Importantly, all of the biological effects of Puf, as well as its effects on dMyc abundance and turnover, are abolished by point mutations in the highly conserved Puf USP catalytic domain. We surmise that Puf stabilizes Myc through its function as a deubiquitylating enzyme that antagonizes the activity of the Ago ubiquitin ligase, previously shown to target Myc for ubiquitylation and degradation (Moberg et al., 2004). Importantly, increased Puf exacerbates, and decreased Puf suppresses, the effect of Ago heterozygotes in enhancing the GMM phenotype. The notion that Puf and Ago act as antagonists receives further support from our findings that Puf protein physically associates with both dMyc and Ago *in vivo*. Interactions between DUBs and their antagonistic E3 ligases, as well as their substrates have been reported previously (Popov et al., 2007b; Sowa et al., 2009). The ability of both the Puf short and long isoforms (Fig. 1A) to modify the dMyc-mediated eye phenotype, and stabilize dMyc and Ago proteins in an ubiquitylation

domain-dependent manner suggests that domain(s) required for Puf to interact with dMyc or Ago are located in a region N-terminal to the core catalytic domain.

We have also found that Puf stabilizes CycE, another known Ago substrate, suggesting that Puf antagonizes Ago function in regulating other targets that are crucial for cell cycle control (Nakayama and Nakayama, 2006). Indeed, flies homozygous for *puf* and *ago* double mutations do not survive, raising the possibility that, in addition to regulating common substrates, they each possess unique targets, as shown for other ubiquitin ligases and DUBs (Komander et al., 2009). Notch would be another potential candidate for Puf activity (Moberg et al., 2004); however, we have failed to find a significant effect of Puf on Notch levels in wing discs (data not shown).

In mammalian cells, the ubiquitin-specific protease USP28 was demonstrated to regulate the turnover of c-Myc by binding and antagonizing the activity of Fbw7α, the vertebrate ortholog of Ago (Popov et al., 2007b). However, Puf and USP28 are not homologs: they appear to be two very distinct USPs in terms of their overall size and amino acid sequence similarity in both their core enzymatic domains and the protein sequence as a whole. The closest mammalian homolog of Puf is USP34 (3546aa) (Quesada et al., 2004). Puf and USP34 are highly homologous in their core catalytic domains (67% identity; 80% similarity) with the catalytic triad conserved, whereas the overall similarity between the two proteins is ~52% (~37% identity).

Previous studies have shown that multiple signaling pathways regulate Ago and Fbw7 expression and activity (Nicholson et al., 2011). Here, we find that Ago levels are increased upon dMyc, as well as upon Puf overexpression. Although the mechanisms by which dMyc and Puf regulate Ago expression are unclear, dMyc-dependent Ago expression may provide a mechanism for dMyc autoregulation (Goodliffe et al., 2005), whereas Puf may stabilize Ago by deubiquitylating it. Indeed, Fbw7 has been shown to be regulated through ubiquitylation (Min et al., 2012). A similar type of dynamic relationship has been reported for the ubiquitin ligase Mdm2 and deubiquitylase HAUSP/USP7 in regulating the stability and function of the tumor suppressor p53 (Brooks and Gu, 2011). Taken together, our data suggest that Ago and Puf represent a regulatory node that controls degradation of Myc and CycE (as summarized in Fig. 7J), and very likely other growth control factors. Further studies will be required to identify additional substrates of Puf and to understand the physiological importance of Puf-mediated regulation of protein degradation in *Drosophila*.

MATERIALS AND METHODS

Drosophila stocks

All the fly stocks were maintained at 22-25°C on standard medium unless otherwise specified. Temperature-inducible experiments were carried out by maintained crosses at 18°C until they were shifted to 29°C for indicated duration.

The transgenic lines *UAS-puf^{WT}*, *UAS-puf^{CA}*, *UAS-puf$^{CA/HA}$*, *UAS-puf^{WT-S}*, *UAS-puf$^{CA/HA-S}$* and *UAS-ash2* were generated for this study. Fly stocks used were: *w^{1118}* (wild type), *UAS-dMyc*, *EP(3)3472*, *EY03971* and *CG5794^{A459}*; *UAS-dMycRNAi* (VDRC, KK106066), *UAS-pufRNAi* (VDRC, GD27517 and KK106192), *GMM (GMR-Gal4, UAS-dMyc^{132}/CyO; UAS-dMyc^{42}, UAS-dMyc^{13}); ap-Gal4,UAS-GFP, GDK (GMR-Gal4, UAS-CycD UAS-Cdk4/CyO), UAS-cycE* and *UAS-diap1* (gifts from Dr B. Edgar, University of Heidelberg, Germany); *ago^{1}*, *ago^{4}*, *UAS-ago* (a gift from Dr K. H. Moberg, Emory University School of Medicine, Atlanta, GA, USA), *UAS-agoRNAi* (#31501, BDSC), *tub-Gal4; tub-Gal80^{ts}, ci-Gal4; tub-Gal80^{ts}* and *ap-Gal4; tub-Gal80^{ts}*. Gal4 drivers obtained from BDSC were: *GMR-Gal4, act-Gal4*, *dpp-Gal4, Bx$^{MS1096-KE}$-Gal4, en-Gal4, rn-Gal4* and *A9-Gal4*.

Cloning and generation of transgenic flies

For long-isoform *puf*, PCR primers specific for *puf-RD* was used to amplify *puf* cDNA. Site-directed mutagenesis was used to generate *puf^{CA}* and *puf$^{CA/HA}$* clones. All full-length cDNA clones were subcloned into the *Eco*RI site of the pUAST vector, and verified by sequencing. The short isoform of *puf* cDNA, (*puf-RE*) was generated by replacing C-terminal region of the long-isoform *puf* cDNA with the *Stu*I-*Not*I fragment from cDNA clone AT30546 (BDGP). *UAS-ash2* transgenic flies were generated by cloning the full-length *ash2* ORF (clone LD31690 from BDGP). All transgenic flies were generated by Bestgene. Primer sequences used for cloning and quantitative validation of gene expression are listed in supplementary material Tables S1 and S2.

Puf antibody production

Rabbit polyclonal antisera were generated using peptides composed of amino acids 13-181 (anti-PufN) or peptides composed of amino acids 3667-3912 (anti-PufC). Specificity of both anti-Puf antisera was confirmed on *puf* mutant, *puf^{A459}* and RNAi knockdown strains.

Antibodies

The following primary antibodies were used: rabbit anti-Puf (1:2000), mouse anti-dMyc (1:10), rabbit monoclonal anti-cleaved caspase 3 (1:100, Cell Signaling, #9664), mouse anti-lamC (1:50, DSHB), guinea pig anti-Ago (1:2000, a gift from Dr K. H. Moberg). Alexa Fluor-conjugated secondary antibodies (1:1000) were from Molecular Probes. Samples were analyzed on a Nikon Eclipse Ti or a Zeiss LSM510 confocal microscope. Western blotting was carried out as previously described (Secombe et al., 2007), Primary antibodies used were: anti-dMyc 1:500, anti-tubulin 1:5000 (Sigma), anti-Puf 1:10,000 and guinea pig anti-Ago 1:10,000 (Mortimer and Moberg, 2007).

Immunoprecipitation

Immunoprecipitations were performed by dissecting discs from wandering 3rd instar larvae (75 discs per sample in overexpression larvae, 150 discs per sample in endogenous larvae) and placing them in PBS with Complete protease inhibitor cocktail (Roche). Discs were lysed in 1 volume of RIPA buffer with inhibitors. Lysate was cleared by centrifugation and diluted to 1 ml with PBS plus inhibitors. Protein was precleared for 1 hour with a combination of protein A/G beads (Invitrogen). Protein was then incubated with antibody diluted to 1:10 for 4 hours, and added to 50 µl protein A/G beads overnight. Immunoprecipitations were washed with PBS plus inhibitors five times, resuspended with Laemmli buffer, and run on a precast gradient gel.

In situ hybridization

Antisense RNA probes were generated using cDNA clones (*ash2* LD31680, *puf* AT30546, *CG31125* SD02419, *CG6695* SD06668, *wsck* LD25626, *atl* GH09383 and *syx18* LD37002) (BDGP). cDNAs were linearized with appropriate restriction enzymes and purified with Qiagen PCR Purification Kit. Hybridization was carried out as described previously (Kozopas et al., 1998). Anti-DIG antibody (Roche) was used at a concentration of 1:4000.

Electron microscopy

Scanning electron microscopy (SEM) and transmission electron microscopy (TEM) were performed on a JEOL 1230 microscope with *Drosophila* eyes prepared as described (http://sharedresources.fhcrc.org/sites/default/files/EMProceduresManual.pdf).

Acknowledgements

We thank Dr Laura Buttitta and members of the Eisenman Lab for comments and suggestions; Dr Bruce A. Edgar and Dr Kenneth H. Moberg for reagents; Vienna *Drosophila* RNAi Center, Bloomington *Drosophila* Stock Center and the TRiP at Harvard Medical School (NIH/NIGMS R01-GM084947) for fly stocks; the Developmental Studies Hybridoma Bank for antibodies; and Berkeley *Drosophila* Genome Project for cDNA clones.

Competing interests

The authors declare no competing financial interests.

Author contributions

R.N.E. was principal investigator for this work. R.N.E. and L.L. wrote the manuscript. L.L. and S.A. performed the experiments. J.S. devised the original screen.

Funding

This work was supported by the National Cancer Institute/National Institutes of Health [R37CA57138 to R.N.E.]. Deposited in PMC for release after 12 months.

Supplementary material

Supplementary material available online at
http://dev.biologists.org/lookup/suppl/doi:10.1242/dev.096941/-/DC1

References

Bellen, H. J., Levis, R. W., Liao, G., He, Y., Carlson, J. W., Tsang, G., Evans-Holm, M., Hiesinger, P. R., Schulze, K. L., Rubin, G. M. et al. (2004). The BDGP Gene Disruption Project. *Genetics* **167**, 761-781.

Bellosta, P. and Gallant, P. (2010). Myc function in drosophila. *Genes & Cancer* **1**, 542-546.

Bhat, K. P. and Greer, S. F. (2011). Proteolytic and non-proteolytic roles of ubiquitin and the ubiquitin proteasome system in transcriptional regulation. *Biochim. Biophys. Acta* **1809**, 150-155.

Brooks, C. L. and Gu, W. (2011). p53 regulation by ubiquitin. *FEBS Lett.* **585**, 2803-2809.

Brooks, C. L., Li, M., Hu, M., Shi, Y. and Gu, W. (2007). The p53-Mdm2-HAUSP complex is involved in p53 stabilization by HAUSP. *Oncogene* **26**, 7262-7266.

Clague, M. J., Coulson, J. M. and Urbé, S. (2012). Cellular functions of the DUBs. *J. Cell Sci.* **125**, 277-286.

Dang, C. V. (2012). MYC on the path to cancer. *Cell* **149**, 22-35.

Datar, S. A., Jacobs, H. W., de la Cruz, A. F. A., Lehner, C. F. and Edgar, B. A. (2000). The Drosophila cyclin D-Cdk4 complex promotes cellular growth. *EMBO J.* **19**, 4543-4554.

de Bie, P. and Ciechanover, A. (2011). Ubiquitination of E3 ligases: self-regulation of the ubiquitin system via proteolytic and non-proteolytic mechanisms. *Cell Death Differ.* **18**, 1393-1402.

Dickson, B., Dietzl, G., Keleman, K.; VDRC project members (2007). RNAi construct and insertion data submitted by the Vienna Drosophila RNAi Center. FlyBase, FBrf0200327.

Flockhart, I., Booker, M., Kiger, A., Boutros, M., Armknecht, S., Ramadan, N., Richardson, K., Xu, A., Perrimon, N. and Mathey-Prevot, B. (2006). FlyRNAi: the drosophila RNAi screening center database. *Nucleic Acids Res.* **34**, D489-D494.

Gallant, P. (2006). Myc/Max/Mad in invertebrates – the evolution of the Max network. *Curr. Top. Microbiol. Immunol.* **302**, 235-253.

Gallant, P. (2009). Drosophila Myc. In *Advances in Cancer Research*, Vol. 103 (ed. F. V. W. George and K. George), pp. 111-144. Academic Press.

Gallant, P., Shiio, Y., Cheng, P. F., Parkhurst, S. M. and Eisenman, R. N. (1996). Myc and Max homologs in Drosophila. *Science* **274**, 1523-1527.

Galletti, M., Riccardo, S., Parisi, F., Lora, C., Saqcena, M. K., Rivas, L., Wong, B., Serra, A., Serras, F., Grifoni, D. et al. (2009). Identification of domains responsible for ubiquitin-dependent degradation of dMyc by glycogen synthase kinase 3β and casein kinase 1 kinases. *Mol. Cell. Biol.* **29**, 3424-3434.

Goodliffe, J. M., Wieschaus, E. and Cole, M. D. (2005). Polycomb mediates Myc autorepression and its transcriptional control of many loci in Drosophila. *Genes Dev.* **19**, 2941-2946.

Grandori, C., Cowley, S. M., James, L. P. and Eisenman, R. N. (2000). The Myc/Max/Mad network and the transcriptional control of cell behavior. *Annu. Rev. Cell Dev. Biol.* **16**, 653-699.

Hann, S. R. (2006). Role of post-translational modifications in regulating c-Myc proteolysis, transcriptional activity and biological function. *Semin. Cancer Biol.* **16**, 288-302.

Herranz, H. and Milán, M. (2008). Signalling molecules, growth regulators and cell cycle control in Drosophila. *Cell Cycle* **7**, 3335-3337.

Hu, M., Gu, L., Li, M., Jeffrey, P. D., Gu, W. and Shi, Y. (2006). Structural basis of competitive recognition of p53 and MDM2 by HAUSP/USP7: Implications for the regulation of the p53–MDM2 pathway. *PLoS Biol.* **4**, e27.

Johnston, L. A., Prober, D. A., Edgar, B. A., Eisenman, R. N. and Gallant, P. (1999). Drosophila myc regulates cellular growth during development. *Cell* **98**, 779-790.

Koepp, D. M., Schaefer, L. K., Ye, X., Keyomarsi, K., Chu, C., Harper, J. W. and Elledge, S. J. (2001). Phosphorylation-dependent ubiquitination of cyclin E by the SCFFbw7 ubiquitin ligase. *Science* **294**, 173-177.

Komander, D., Clague, M. J. and Urbe, S. (2009). Breaking the chains: structure and function of the deubiquitinases. *Nat. Rev. Mol. Cell Biol.* **10**, 550-563.

Kozopas, K. M., Samos, C. H. and Nusse, R. (1998). DWnt-2, a drosophila Wnt gene required for the development of the male reproductive tract, specifies a sexually dimorphic cell fate. *Genes Dev.* **12**, 1155-1165.

Liu, J. and Levens, D. (2006**).** Making Myc. *Curr. Top Microbiol. Immunol.* **302**, 1-32.

Maines, J. Z., Stevens, L. M., Tong, X. and Stein, D. (2004). Drosophila dMyc is required for ovary cell growth and endoreplication. *Development* **131**, 775-786.

Mandal, S., Freije, W. A., Guptan, P. and Banerjee, U. (2010). Metabolic control of G1–S transition: cyclin E degradation by p53-induced activation of the ubiquitin–proteasome system. *J. Cell Biol.* **188**, 473-479.

Min, S.-H., Lau, A. W., Lee, T. H., Inuzuka, H., Wei, S., Huang, P., Shaik, S., Lee, D. Y., Finn, G., Balastik, M. et al. (2012). Negative regulation of the stability and tumor suppressor function of Fbw7 by the Pin1 prolyl isomerase. *Mol. Cell* **46**, 771-783.

Moberg, K. H., Bell, D. W., Wahrer, D. C. R., Haber, D. A. and Hariharan, I. K. (2001). Archipelago regulates cyclin E levels in drosophila and is mutated in human cancer cell lines. *Nature* **413**, 311-316.

Moberg, K. H., Mukherjee, A., Veraksa, A., Artavanis-Tsakonas, S. and Hariharan, I. K. (2004). The drosophila F box protein archipelago regulates dMyc protein levels in vivo. *Curr. Biol.* **14**, 965-974.

Montagne, J., Stewart, M. J., Stocker, H., Hafen, E., Kozma, S. C. and Thomas, G. (1999). Drosophila S6 kinase: A regulator of cell size. *Science* **285**, 2126-2129.

Montero, L., Müller, N. and Gallant, P. (2008). Induction of apoptosis by drosophila Myc. *Genesis* **46**, 104-111.

Mortimer, N. T. and Moberg, K. H. (2007). The drosophila F-box protein archipelago controls levels of the trachealess transcription factor in the embryonic tracheal system. *Dev. Biol.* **312**, 560-571.

Müller, J. and Eilers, M. (2009). Ubiquitination of Myc: proteasomal degradation and beyond. In *The Ubiquitin System in Health and Disease*, Vol. 2008/1 (ed. S. Jentsch and B. Haendler), pp. 99-113. Berlin, Heidelberg: Springer.

Nakayama, K. I. and Nakayama, K. (2006). Ubiquitin ligases: cell-cycle control and cancer. *Nat. Rev. Cancer* **6**, 369-381.

Nicholson, S. C., Nicolay, B. N., Frolov, M. V. and Moberg, K. H. (2011). Notch-dependent expression of the archipelago ubiquitin ligase subunit in the Drosophila eye. *Development* **138**, 251-260.

Orme, M. and Meier, P. (2009). Inhibitor of apoptosis proteins in drosophila: gatekeepers of death. *Apoptosis* **14**, 950-960.

Parisi, F., Riccardo, S., Daniel, M., Saqcena, M., Kundu, N., Pession, A., Grifoni, D., Stocker, H., Tabak, E. and Bellosta, P. (2011). Drosophila insulin and target of rapamycin (TOR) pathways regulate GSK3 beta activity to control Myc stability and determine Myc expression in vivo. *BMC Biol.* **9**, 65.

Pierce, S. B. (2004). dMyc is required for larval growth and endoreplication in drosophila. *Development* **131**, 2317-2327.

Popov, N., Herold, S., Llamazares, M., Schülein, C. and Eilers, M. (2007a). Fbw7 and Usp28 regulate Myc protein stability in response to DNA damage. *Cell Cycle* **6**, 2327-2331.

Popov, N., Wanzel, M., Madiredjo, M., Zhang, D., Beijersbergen, R., Bernards, R., Moll, R., Elledge, S. J. and Eilers, M. (2007b). The ubiquitin-specific protease USP28 is required for MYC stability. *Nat. Cell Biol.* **9**, 765-774.

Prober, D. A. and Edgar, B. A. (2001). Growth regulation by oncogenes-new insights from model organisms. *Curr. Opin. Genet. Dev.* **11**, 19-26.

Quesada, V. c., Díaz-Perales, A., Gutiérrez-Fernández, A., Garabaya, C., Cal, S. and López-Otín, C. (2004). Cloning and enzymatic analysis of 22 novel human ubiquitin-specific proteases. *Biochem. Biophys. Res. Commun.* **314**, 54-62.

Reyes-Turcu, F. E., Ventii, K. H. and Wilkinson, K. D. (2009). Regulation and cellular roles of ubiquitin-specific deubiquitinating enzymes. *Annu. Rev. Biochem.* **78**, 363-397.

Riemer, D., Stuurman, N., Berrios, M., Hunter, C., Fisher, P. A. and Weber, K. (1995). Expression of drosophila lamin C is developmentally regulated: analogies with vertebrate A-type lamins. *J. Cell Sci.* **108**, 3189-3198.

Rorth, P., Szabo, K., Bailey, A., Laverty, T., Rehm, J., Rubin, G. M., Weigmann, K., Milan, M., Benes, V., Ansorge, W. et al. (1998). Systematic gain-of-function genetics in drosophila. *Development* **125**, 1049-1057.

Secombe, J., Pispa, J., Saint, R. and Richardson, H. (1998). Analysis of a drosophila cyclin E hypomorphic mutation suggests a novel role for cyclin E in cell proliferation control during eye imaginal disc development. *Genetics* **149**, 1867-1882.

Secombe, J., Li, L., Carlos, L. and Eisenman, R. N. (2007). The trithorax group protein lid is a trimethyl histone H3K4 demethylase required for dMyc-induced cell growth. *Genes Dev.* **21**, 537-551.

Sheng, Y., Saridakis, V., Sarkari, F., Duan, S., Wu, T., Arrowsmith, C. H. and Frappier, L. (2006). Molecular recognition of p53 and MDM2 by USP7/HAUSP. *Nat. Struct. Mol. Biol.* **13**, 285-291.

Sowa, M. E., Bennett, E. J., Gygi, S. P. and Harper, J. W. (2009). Defining the human deubiquitinating enzyme interaction landscape. *Cell* **138**, 389-403.

Steller, H. (2008). Regulation of apoptosis in drosophila. *Cell Death Differ.* **15**, 1132-1138.

Thomas, L. R. and Tansey, W. P. (2011). Proteolytic control of the oncoprotein transcription factor Myc. In *Advances in Cancer Research*, Vol. 110 (ed. K. George), pp. 77-106. Academic Press.

Tsou, W.-L., Sheedlo, M. J., Morrow, M. E., Blount, J. R., McGregor, K. M., Das, C. and Todi, S. V. (2012). Systematic analysis of the physiological importance of deubiquitinating enzymes. *PLoS ONE* **7**, e43112.

Tweedie, S., Ashburner, M., Falls, K., Leyland, P., McQuilton, P., Marygold, S., Millburn, G., Osumi-Sutherland, D., Schroeder, A., Seal, R. et al. (2009). FlyBase: enhancing drosophila gene ontology annotations. *Nucleic Acids Res.* **37**, D555-D559.

Varshavsky, A. (2012). The ubiquitin system, an immense realm. *Annu. Rev. Biochem.* **81**, 167-176.

Ventii, K. H. and Wilkinson, K. D. (2008). Protein partners of deubiquitinating enzymes. *Biochem. J.* **414**, 161-175.

Vervoorts, J., Lüscher-Firzlaff, J. and Lüscher, B. (2006). The ins and outs of MYC regulation by posttranslational mechanisms. *J. Biol. Chem.* **281**, 34725-34729.

Wu, D. C. and Johnston, L. A. (2010). Control of wing size and proportions by drosophila Myc. *Genetics* **184**, 199-211.

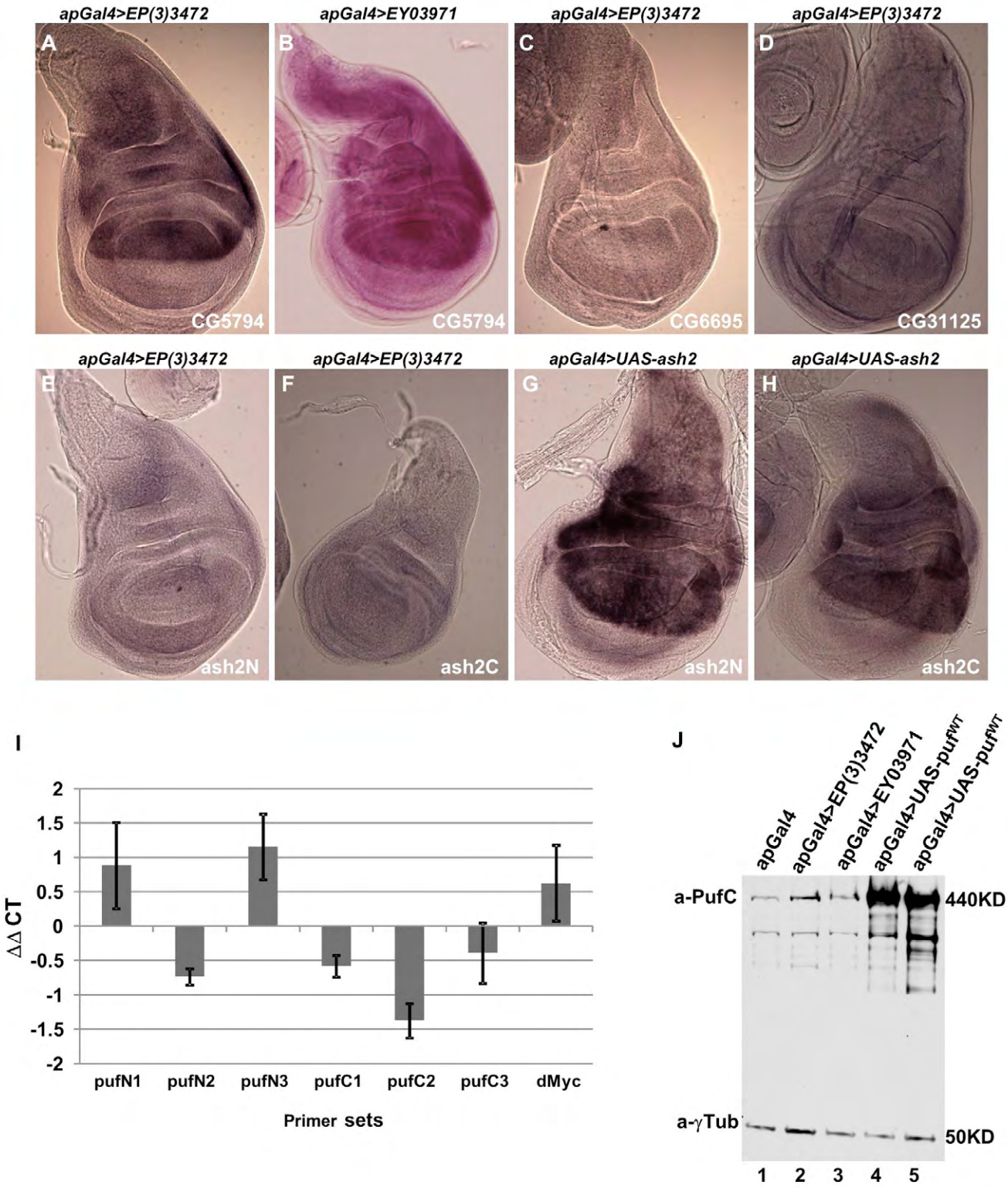

Fig. S1. Activation of *EP(3)3472* and *EY03971* induces *CG5794* expression. (A-F) In situ hybridizations of 3rd instar larval wing discs overexpressing *EP(3)3472* or *EY03971* show only CG5794 expression was induced. (A) *apGal4*; *EP(3)3472* and (B) *apGal4*; *EY03971* induced CG5794 expression. *apGal4*; *EP(3)3472* did not induce CG6695 (C) or CG31125 (D) expression. *apGal4*; *EP(3)3472* did not induce ash2 expression as indicated by anti-sense RNA probe against N-terminal (E) or C-terminal of ash2. (G,H) *apGal4*; *UAS-ash2* activated ash2 expression. (I)). qRT-PCR showing detection of puf transcripts in puf mutant (puf^{A495}) using various primers, and puf mutant has no significant effect on dMyc transcript levels. 30 wing discs per genotype were used to isolate mRNA. Relative expression levels (ΔΔCT) were calculated using *RpS16* as internal control. Data represent mean of three biological samples analyzed in duplicate. Error bars reflect standard error of the mean. Transgenes were induced for 20h using temperature inducible Gal4 drivers. (J) Western blot showing *UAS-puf* expressed (lane 4-5) Puf at much higher level than w^{1118} control (lane1), *EP(3)3472* (lane 2) or *EY03971*(lane3). Each lane used protein lysates from 10 wing discs.

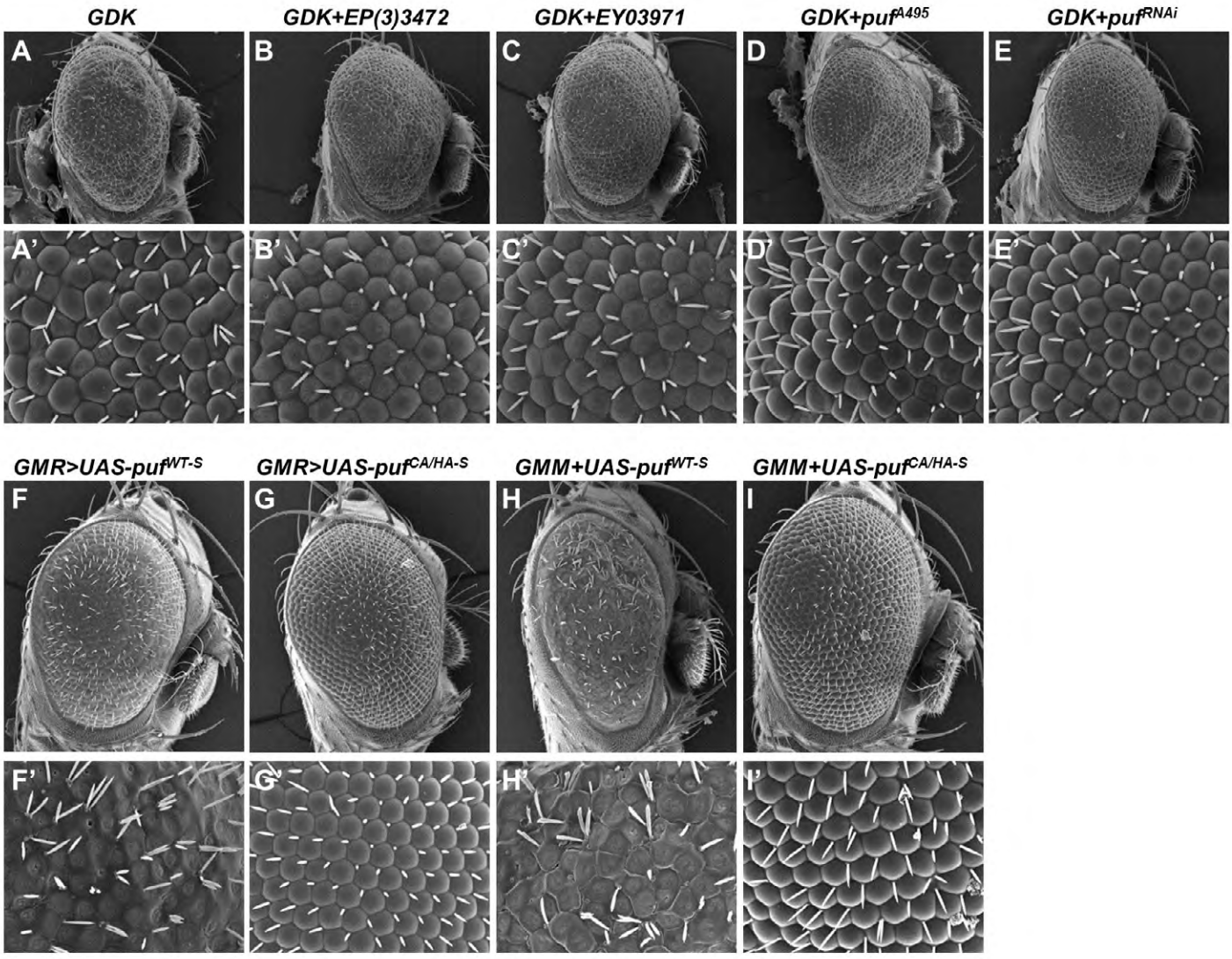

Fig. S2. Puf does not modify GDK dependent eye phenotype. (A-E) Scanning electron micrographs (SEM) of adult compound eyes show that Puf does not modify *GDK (GMR-Gal4, UAS-cycD, UAS-ckd4*) eye phenotype. (F-I) SEM of adult compound eye show that short isoform of Puf functions similarly to the long isoform. (A, A') *GDK*; (B,B') *GDK, EP(3)3472/+*; (C,C') *GDK, EY03971*/+; (D,D') *GDK*, puf^{A459}/+; (E,E') *GDK,UAS-pufRNAi*/+; (F,F') *GMR-Gal4, UAS-*puf^{WTS}/+; (G,G') *GMR-Gal4,UAS-*$puf^{CA/HAS}$/+; (H,H') *GMM,UAS-*puf^{WTS}/+; (I,I) *GMM, UAS-*$puf^{CA/HAS}$/+. SEM magnification for (A-I) is 160x and 750x for (A'-I')

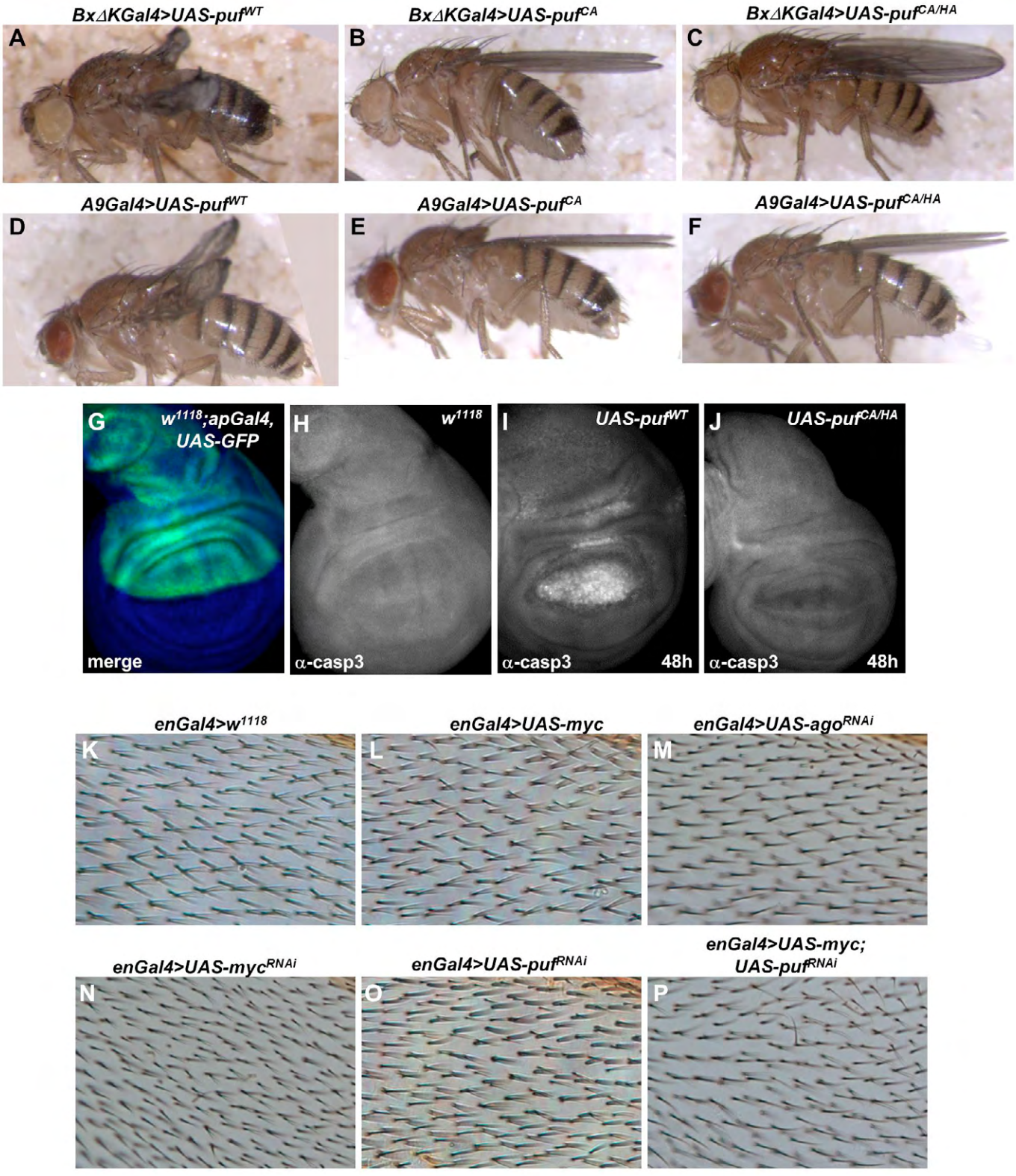

Fig. S3. Puf is necessary for cell growth in the wing. (A-F) *UAS-puf* induced wing phenotype depends on its catalytic activity. (G-J) *UAS-puf* induced apoptosis in an enzymatic dependent manner 48h after induction as indicated by cleaved caspase 3 (casp3) staining. (K-P) Reduced dMyc or Puf levels resulted in smaller cell size as demonstrated by increased density of the bristles. (A*) BxDKGal4, UAS-puf*^{WT}; (B) *BxDKGal4,UAS-puf*^{CA}; (C) *BxDKGal4,UAS-puf*$^{CA/HA}$; (D) *A9Gal4,UAS-puf*^{WT}; (E*) A9-Gal4,UAS-puf*^{CA}; (F) *A9Gal4,UAS-puf*$^{CA/HA}$. (G,H) *w*^{1118}*, apGal4, UAS-GFP* control*;* (I) *apGal4,UAS-puf*^{WT}; (J) *apGal4,UAS-puf*$^{CA/HA}$; (K) *w*^{1118}*, enGal4* control; (L) *enGal4,UAS-dMyc*; (M) *enGal4,UAS-agoRNAi;* (N) *enGal4,UAS-MycRNAi*; (O) *enGal4,UAS-pufRNAi*(KK)*;* (P) *enGal4,UAS-dMyc,UAS-pufRNAi*.

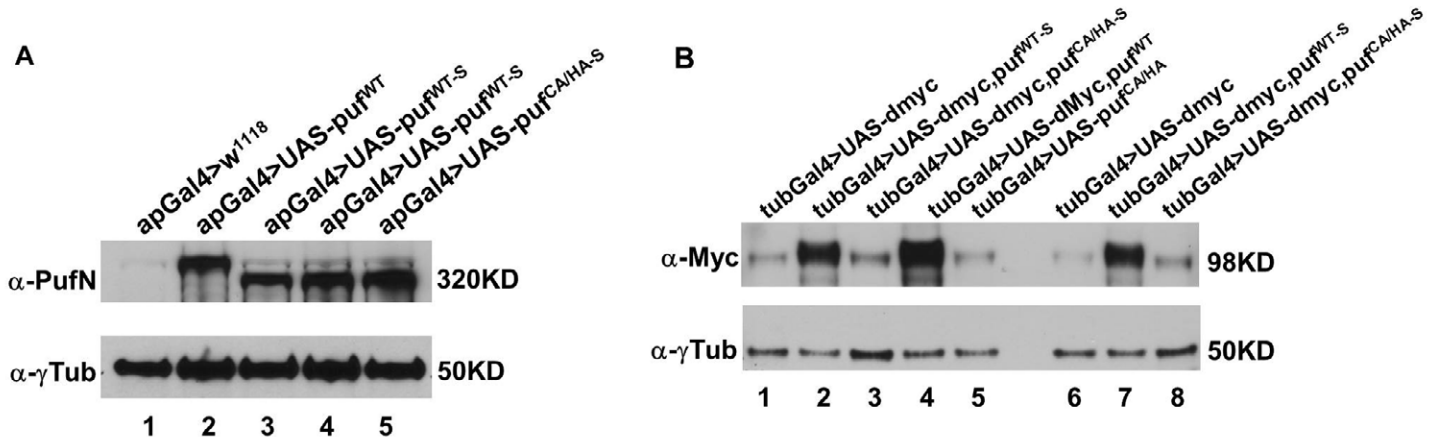

Fig. S4. Short isoform of Puf affects dMyc levels. (A) Western blot shows short isoform of Puf transgenes *UAS-puf*$^{WT-S}$ and *UAS-puf*$^{CA/HA-S}$ (lanes 3-5) expressed at similar levels as the long isoform *UAS-puf*^{WT}(lane 2). (B) Both long (lanes 4,5) and short isoforms (lane 2,3,7,8) of Puf regulate dMyc levels dependent on a WT catalytic domain. Protein lysates form 10 wing discs were used for each lane. All transgenes were induced for 18h using temperature inducible Gal4 drivers.

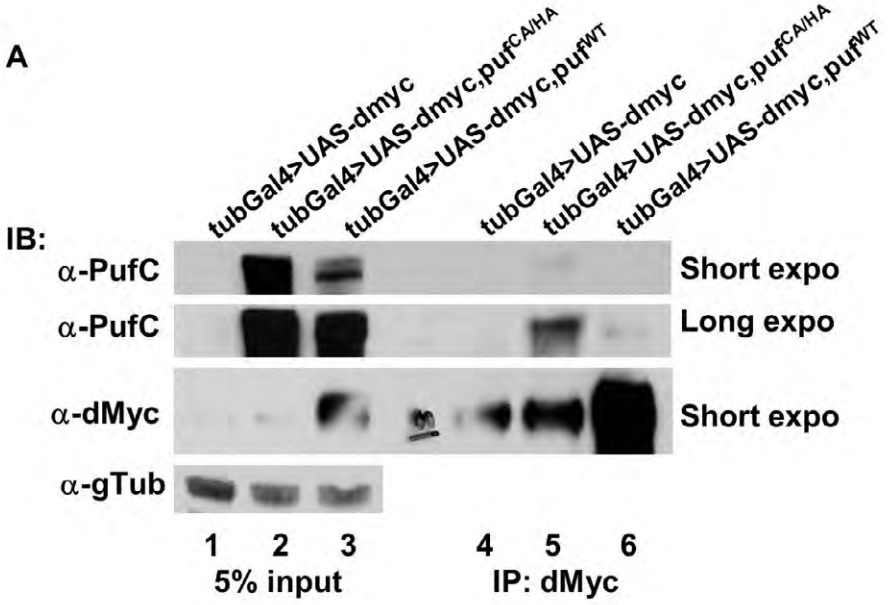

Fig. S5. dMyc and Puf form a protein complex. (A) Co-IP showing that both Puf^{WT} (lane 5) and Puf$^{CA/HA}$ (lane 6) form a protein complex with dMyc *in vivo*. (Lanes 1-3) Input for each genotype. Protein lysates isolated from wing discs of 3rd instar larvae overexpressing dMyc and dMyc+Puf^{WT} or dMyc+Puf$^{CA/HA}$ were immunoprecipitated with anti-dMyc antisera and analyzed by western blots using anti-PufC.

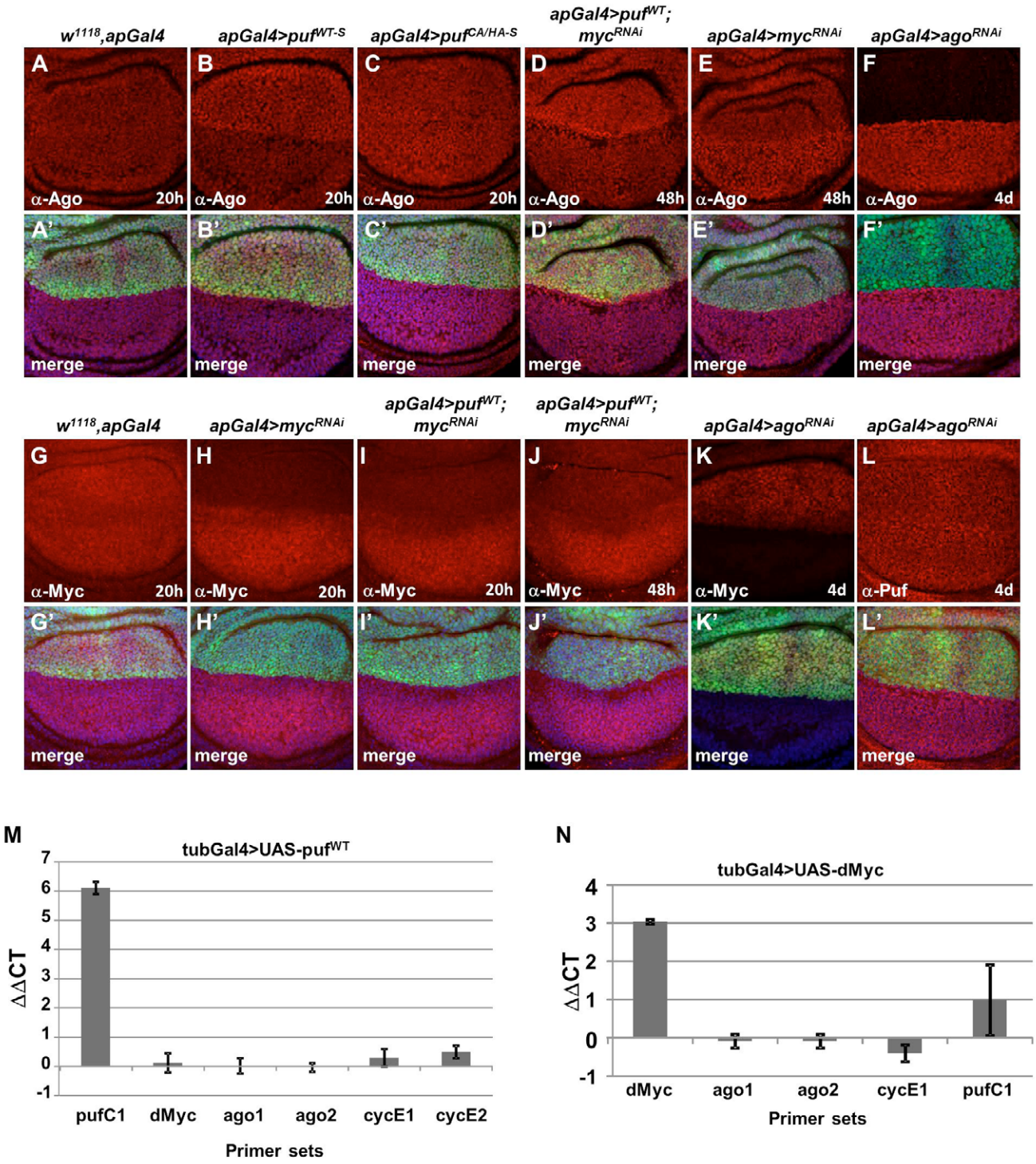

Fig. S6. Ago levels are regulated by Puf and dMyc. (A-C) Immunostaining of the 3rd instar larval wing disc 20 hours after induction showing Puf and dMyc regulate Ago levels. Transgene expression is marked by GFP. (A, A') *w*^{1118}*,ap-Gal4,UAS-GFP* serves as control showing Ago expression pattern. (B,B') effect of wildtype Puf short isoform (*ap-Gal4, UAS-GFP, UAS-puf*$^{WT\text{-}S}$) on endogenous Ago. (C,C') effect of short isoform of enzymatic inactive Puf (*ap-Gal4,UAS-GFP,UAS-puf*$^{CA/HA\text{-}S}$) on endogenous Ago. (D-E) Immunostaining of the 3rd instar larval wing disc showing Puf and dMyc regulate Ago levels 48 hours after induction of transgene. (D,D') Knockdown of *dmyc* (*ap-Gal4, UAS-GFP, UAS-dmyc*^{RNAi}); (E,E') induction of Puf in the presence of *dmyc* knockdown (*ap-Gal4, UAS-GFP, dmyc*^{RNAi}*,UAS-puf*^{WT}). (F,F) Immunostaining of the 3rd instar larval wing disc showing reduced Ago levels after *ago* RNAi knockdown (*ap-Gal4,UAS-GFP,UAS-ago*^{RNAi}). (G,G') *w*^{1118}*,ap-Gal4,UAS-GFP* serves as control showing *dmyc* expression pattern. (H-J) Effect of *dmyc* knockdown by induction of *dmyc*RNAi transgene at various time points (*ap-Gal4,UAS-GFP,UAS-dmyc*^{RNAi}). (K-L) Effect of *ago* knockdown (*ap-Gal4,UAS-GFP,UAS-ago*^{RNAi}) on endogenous dMyc (K.K') or Puf (L,L'). (M) qRT-PCR showing Puf overexpression has no effect on *dmyc*, *ago* and *cycE* transcript levels. (N) qRT-PCR showing dMyc overexpression has no effect on *ago*, *cycE* and *puf* transcript levels. Relative expression levels (ΔΔCT) were calculated using *RpS16* as internal control. Data represent mean of three biological samples analyzed in duplicate. Error bars reflect standard error of the mean. Transgenes were induced for 20h using temperature inducible Gal4 drivers.

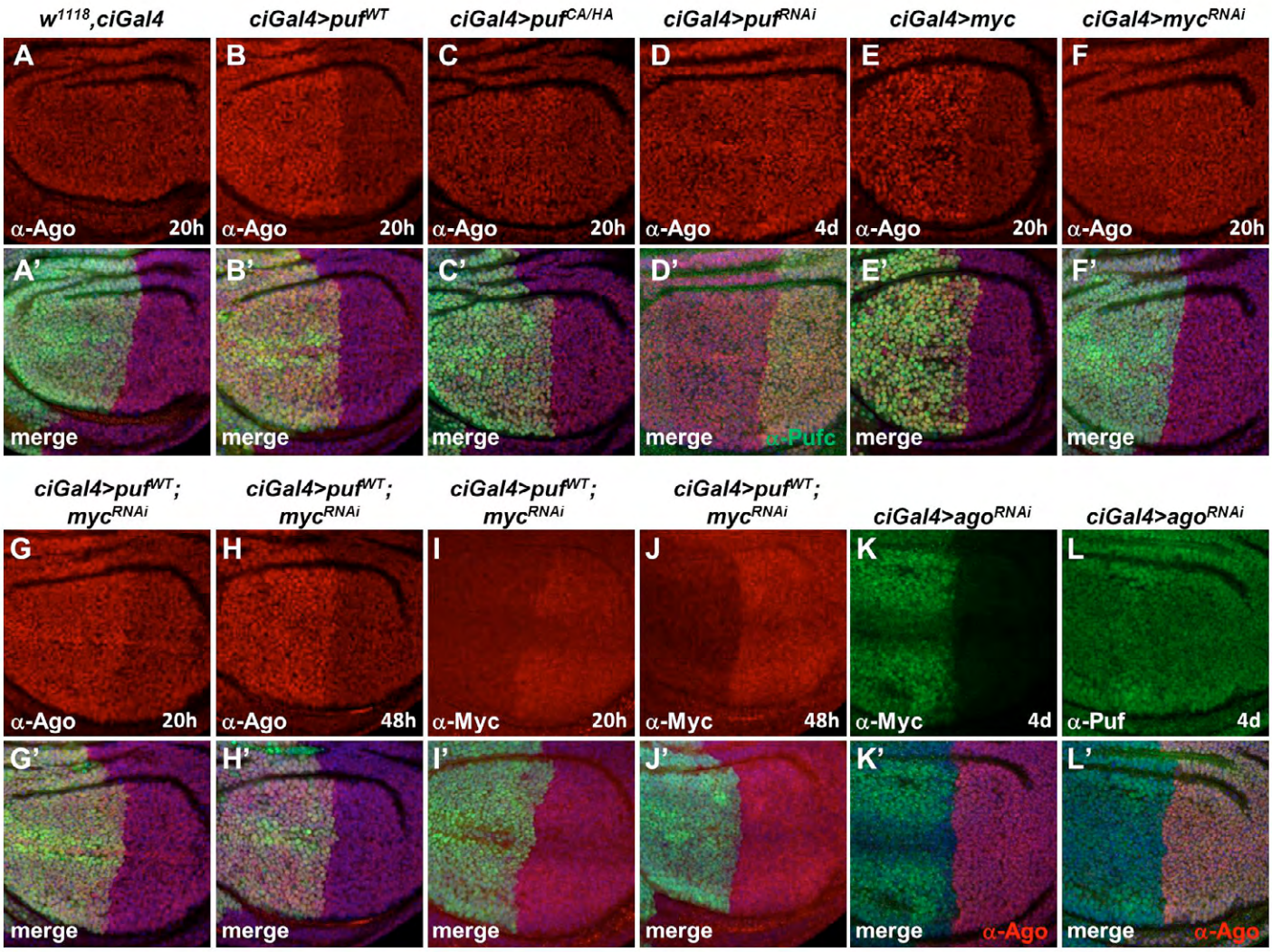

Fig. S7. Ago levels are regulated by Puf and dMyc. (A-H) Immunostaining of the 3rd instar larval wing disc showing Puf and dMyc regulate Ago levels. (A, A') *w*^{1118}*,ci-Gal4,UAS-GFP* serves as control showing Ago expression pattern. (B,B') effect of wildtype Puf (*ci-Gal4, UAS-GFP, UAS-puf*^{WT}) on endogenous Ago. (C,C') effect of enzymatic inactive Puf (*ci-Gal4,UAS-GFP,UAS-puf*$^{CA/HA}$) on endogenous Ago. (D,D') effect of Puf knockdown (marked by anti-PufC) on Ago (*ci-Gal4, UAS-puf*^{RNAi}). (E,E') effect of dMyc overexpression on Ago (*ci-Gal4, UAS-GFP, UAS-dmy)*. (F,F') effect of dMyc knockdown on Ago (*ci-Gal4, UAS-GFP, UAS-dmyc*^{RNAi}). (G-J) effect of Puf overexpression in the presence of dMyc knockdown (*ci-Gal4, UAS-GFP, UAS-puf*^{WT}*, dmyc*^{RNAi}) on Ago (G,H) and dMyc (I,J) at indicated time points. (K-L) effects of ago knockdown (*ci-Gal4,UAS-GFP,UAS-ago*^{RNAi}) on endogenous dMyc (K.K') or Puf (L,L').

Table S1. Primers used for cloning

Primers for *puf* wildtype cloning		
	Forward	**Reverse**
N-terminal	CATCCTAAATGGCATTGCAC	CCACATCCATCAGATCGACA
Mid 1	GCAAAAAGACGAGCAACAAG	CCACTACCGAAAGTGCTGGT
Mid 2	GTAAATCCCCAGCACCACAC	CTGCAGATGCTCTGGCAGTC
Mid 3	CACTTTTCCTTTCCGCTACG	ATCAGCGTGGACCAAGAGAC
C-terminal	CCCTCAATCCGCACAGTTAT	CTAAATCTGTGTTGGACTTGCCG
C-terminal NdeI site		CCATTATGAATCTGTGTTGGAC TTGCCGCCT

Primers for *puf* catalytic mutations		
	Forward	**Reverse**
Cys-Ala	CTAATTTGGGAGCCACTGCC TATATGGCCTCTTGCG	ACGCAAGAGGCCATATAGG CAGTGGCTCCCAAATTA
His 1-Ala	CTGGTGGGCGTCACTGTCGC CACGGGCACAGCGGATGG	CCATCCGCTGTGCCCGTG GCGACAGTGACGCCCACCAG
His 2-Ala	CGCCACGGGCACAGCGGC TGGCGGCGCCTACTACAGC TTTATAAAGG	CCTTTATAAAGCTGTAGT AGGCGCCGCCAGCCGCTG TGCCCGTGGCG

Table S2. Quantitative real-time PCR primers

Primer sequences from IDT (http://www.idtdna.com/site) were as follows.

	Primers for RT-PCR	
	Forward	Reverse
RpS16	CTGGAGCCAGTTCTGCTTCT	TCTCCTTCTTGGAAGCCTCA
CamKII	AAGCAAGGACATGCACATACC	GCAGATGCACTTCGATGAAA
pufN1	CAAGAGCCTGGTCGACTTCT	CATCTTCTCCACGGACAGC
pufN2	AACCAAATGGTGCGTCAAAT	CCTCGTCTGTCTCCACTTCC
pufN3	GCCCAAAGACTTCTCTGCAA	GCGCGTGTATTAAATGCTTTG
pufC1	AACAAGAGCGAGCGGTTTAG	CTGAGGGTGCTCCTTTTCCT
pufC2	CAAATTCTGGGTGGGCATACA	TTCGCTCGTCCCTAAGGACATTG
pufC3	GTCTCTTGGTCCACGCTGAT	CCTCGAAACACATCTCAATGC
Myc1	AGCATCACCACCAACAACAA	GGACCATCGTCCACCATATC
Myc2	CAGTTCCAGTTCGCAGTCAA	AGATAAACGCTGCTGGAGGA
ago1	TGATTACGTGCCTGCAGTTC	GGTGTGACCAACCAAAGTGC
ago2	AAGACGGGCGACTTTATACG	CGACGGCACAAATGAGTTTA
cycE 1	CGACTCGCACATTATCCAAA	CGGGGAAGCTTGAATCCTA
cycE 2	GGCATGGCCAACTATTCCTA	AATCACCTGCCAATCCAGAC